2 (mix)

ATS—16486

f

DEPARTMENT OF ELECTRICAL ENGINEERING

UNIVERSITY OF UTAH

SALT LAKE CITY, UTAH
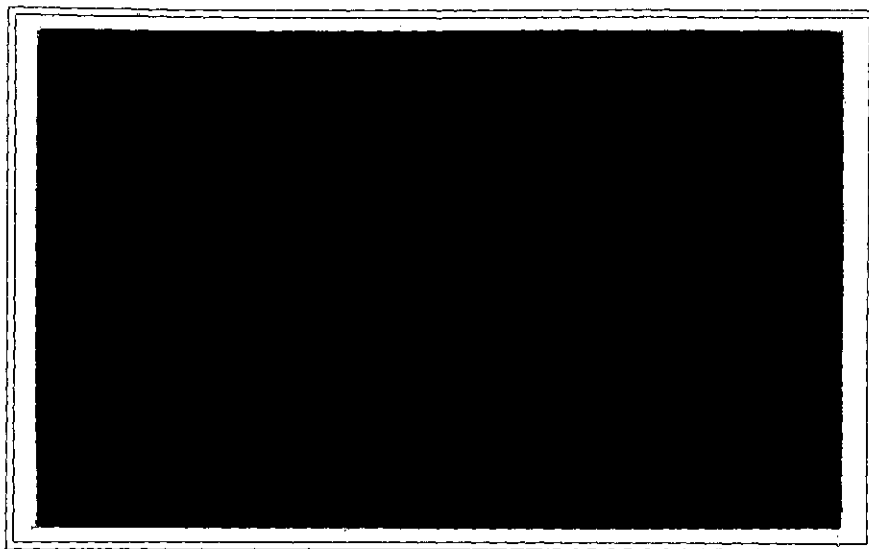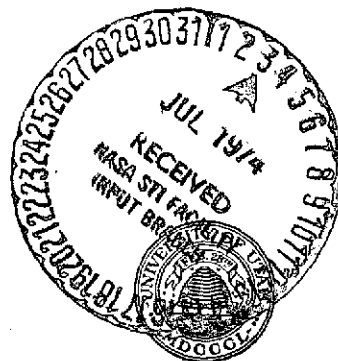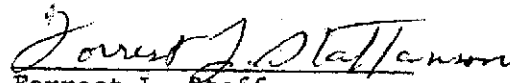
108

SURVEY OF LITERATURE ON CONVECTIVE HEAT TRANSFER COEFFICIENTS AND RECOVERY FACTORS FOR HIGH ATMOSPHERE THERMOMETRY

Progress Report Under
NASA Grant NGR 45-003-025

July 1973

University of Utah
Electrical Engineering Department

Syung Chung
Forrest L. Staffanson

Forrest L. Staffanson
Principal Investigator

i.

FOREWORD

Quantitative knowledge of the convective heat transfer coefficient and thermal recovery factor is essential in the engineering effort to extend the use of immersion thermometric meteorological sensors higher into the upper atmosphere. Such an effort at the University of Utah, sponsored by NASA Langley Research Center (under research grant NGL 45-003-025), has produced an algorithm for the automatic computation of these coefficients. The computer subroutine applies to a variety of sensor types over the varying altitudes and air speeds of rocket-ejected meteorological parachutesondes. A description of the subroutine and tabulated values are presented elsewhere. The authors, in what follows, have adapted and extended the notes of predecessors in the project with the purpose of documenting the underlying bases for the algorithm. Particular acknowledgment is accorded Dr. Sadiq J. Alsaji, now at the College of Engineering Technology, Baghdad, Iraq, for his early contributions to this compilation.

<div align="right">

Forrest L. Staffanson
Principal Investigator

</div>

<div align="center">

i (a)

</div>

TABLE OF CONTENTS

LIST OF SYMBOLS

A	Area
b	Constant (see Eq. 19)
C, Cm	Overheat, mean overheat (see Eq. 31)
Cp, Cv	Specific heats at constant pressure and volume, respectively
D, d	Cylinder or sphere diameter
dVe	Volume element in velocity space
E	Energy flux
F	Measured quantity in dimensionless form (see Eq. 61)
$\overline{F}$	Parameter related to geometry (see Eq. 22)
f	Velocity distribution function
$\overline{G}$	Parameter related to geometry (see Eq. 22)
g	Gravity constant
h	Convective heat transfer coefficient
$\overline{h}$	Average convective heat transfer coefficient
I(s)	Modified Bessel function
ierfc	Integral of complementary error function
Jo	Radiation flow
k	Thermal conductivity
Kn	Knudsen number (see Eq. 1)
L, ℓ	Characteristic length
M	Mach number
m	Mass of molecule
n	Number density
Nu	Nusselt number
$\overline{Nu}$	Average Nusselt number

P	Pressure, or normal component of momentum
Pr	Prandtl number
Q	Heat transfer per unit time
q	Heat transfer per unit time per unit area
R	Radius
$\tilde{R}$	Universal gos constant
Re	Reynolds number
r, r'	Recovery factor, modified recovery factor (see Eq. 64)
St, St'	Stanton number and modified Stanton number (see Eqs. 22 and 30)
T	Temperature
t	Time
$\overline{U}$	Free stream velocity
u	Flow velocity (x-component)
V	Most probable molecular velocity
v	Flow velocity (y-component)
x	Coordinate along the body axis
y	Coordinate normal to surface
α	Thermal accommodation coefficient, or thermal diffusivity $\left(\dfrac{K}{\rho C_p}\right)$
γ	Specific heat ration C_p/C_v
δ, δ'	Tangential and normal momentum accommodation coefficients, respectively
ϵ	Emissivity of the surface
ξ	Molecular velocity
η	Recovery ratio, (T_r/T_o)
η^*	Normalized recovery ratio
θ	Local angle of attack (see Fig. 3)
θ_c	Cone semivertex angle
θ'	$T_1 - T_2$ (see Eq. 70)

λ	Mean free path
μ	Dynamic viscosity
ν	Kinematic viscosity
π	3.14159 .... (= circumference length/diameter)
ρ	Density
σ	Stefan-Boltzmann constant
τ	Tangential component of momentum
ϕ	Modified speed ratio $s \sin \theta$
ψ	Stream function
Ω	Angle for concave surface

SUBSCRIPTS

$a\omega$	Adiabatic wall temperature
c	Continuum flow condition
d	Local condition in cylinder
eq	Equilibrium condition
FM	Free molecule flow condition
in	Incident on surface
ℓ	Average value for characteristic length ℓ
n	Normal component
o	Stagnation condition
re	Reflected from surface
r	Corresponding to recovery (temperature) condition
s	Conditions outside boundary layer in the circular cylinder
ω	Wall condition
x	Local condition

y   Coordinate normal to surface

∞   Free stream condition

1, 2   Denotes two different (surface) conditions

θ   Local angle condition

LIST OF FIGURES

INTRODUCTION

This report concerns heat transfer phenomena of rarefied gas flows, and is based on a literature survey of analytical and experimental rarefied gas dynamics. Subsonic flows are especially emphasized for the purposes of meteorological thermometry in the high atmosphere.

Part one of the report deals with the heat transfer coefficients (in external subsonic rarefied flow) for three basic geometries -- a flat plate, cylinder and sphere -- in all flow regimes; i.e., free molecule flow (Kn > 10), transition flow (10 > Kn > 0.1), slip flow (temperature jump) (0.1 > Kn > 0.01), and continuum flow (Kn > 0.01). Different types of heat transfer phenomena, and the analysis of theoretical and experimental data are presented. The uncertainties calculated from the interpolation rule, $Nu = 1/\left(1/Nu_c + 1/Nu_{FM}\right)$, compared with the available experimental data are also presented for cylinder and sphere.

In part two, recovery factor for each geometry in subsonic rarefied flows is discussed. Uncertainties resulting from analyses of experimental data available at the present time are also presented.

l

PART I

HEAT TRANSFER COEFFICIENT

1. Introduction

The treatment of heat transfer in a gas depends on the structure
of the gas. Normally under standard conditions, the gas is considered
a continuum and no consideration is given to its molecular structure.
In the continuum regime, the flow and heat transfer can be adequately
described in terms of the Reynolds, Mach, Nusselt, and Prandtl numbers.
However, at very low absolute pressures and densities, a gas behaves
more like independent particles described by kinetic theory. Thermo-
metric sensor elements used in the upper atmosphere encounter air flows
throughout the varying degrees of rarefaction between the continuum
and free molecule conditions. The purpose of this report is to survey
the results of recent analytical and experimental investigations of
heat transfer in rarefied gases.

A gas departs from continuum properties and is said to be "rare-
fied" when the molecular mean free path λ approaches 1 percent of the
dimension of the flow field. Suppose ℓ is some characteristic dimen-
sion of the flow field, such as the radius of a cylinder over which the
gas is flowing. The ratio λ/ℓ, Knudsen number [1], is a measure of the
degree of rarefaction of the gas flow. The Knudsen number is related
to the Mach number, $M = V/V_s$, and the Reynolds number, $Re_\ell = \rho V \ell / \mu$.

$$ Kn = \frac{\lambda}{\ell} = \left(\frac{\pi \gamma}{2}\right)^{1/2} \frac{M}{Re_\ell} = 1.49 \frac{M}{Re_\ell} \tag{1} $$

- 2 -

When the Knudsen number is very small, the number of collisions between molecules in the vicinity of the body is large relative to the number of collisions of the molecules with the body. In this case continuum concepts, the Navier-Stokes equations, and the Fourier heat conduction law all apply. Under such conditions the flow is completely characterized by the Reynolds number and Mach number; the Knudsen number does not enter the problem explicitly since it is considered to be small [5].

When Knudsen number becomes sufficiently large, continuum concepts fail and must be modified for calculating the heat transfer. At very high Knudsen number, the number of collisions between molecules becomes negligible and the flow is termed "free molecule flow". Between the continuum and free molecule regimes, there is a rather wide range of intermediate flow regimes.

It is convenient to divide rarefied gas dynamics into the following regimes [1]: free molecule flow (Kn > 10), transition flow (10 > Kn > 0.1), slip flow (0.1 > Kn > 0.01), and continuum flow (Kn < 0.01). The indicated Knudsen number ranges are approximate only, and different types of heat transfer phenomena and theoretical approaches occur in each regime. The following discussion is concerned with understanding the heat transfer mechanisms in the continuum, transition, slip, and free molecular flow regimes for the sphere, cylinder, and flat plate, and is divided into groups based on the different regimes. The analytical and experimental estimation of uncertainty in the heat transfer coefficient for external rarefied subsonic flows around the specified geometries is of particular interest.

2. Continuum Flow Regime

In the continuum regime, the boundary layer concept is used to yield theoretical expressions for heat transfer coefficients. Basic conditions assumed in the development of the boundary layer equations are well observed in continuum flow. Expressions of Nusselt number Nu(re, Pr) available from the literature are briefly discussed below for the flat plate, sphere, and circular cylinder.

2.1. Flat Plate

The boundary layer concept yields theoretical expressions for the heat transfer coefficient over a flat plate. However, the heat transfer coefficient is greatly influenced by the kind of flow, i.e., laminar or turbulent. The heat transfer coefficient with turbulent flow is usually larger than with laminar flow.

2.1.1. Laminar flow over a flat plate

For a flat plate with constant wall temperature heated over its entire length, the boundary layer concept yields the following equation for the local Nusselt number [3]:

$$Nu_x = 0.332 \ (Pr)^{1/3} \left(Re_x\right)^{1/2} \qquad (2)$$

and, therefore, for the convective heat transfer coefficient,

$$h_x = \left(Nu_x\right)\frac{k}{x} = 0.332 \ k \ (Pr)^{1/3} \left(\frac{u}{\nu x}\right)^{1/2} \qquad (3)$$

- 4 -

Often, for calculations in practical problems, an average value h over some length L from the leading edge is useful [3].

$$h = \frac{1}{L} \int_0^L h_x dx = \frac{c}{L} \int_0^L \frac{dx}{\sqrt{x}} = \frac{c}{L} 2 \sqrt{L} = 2 \frac{c}{\sqrt{L}} = 2h_L \qquad (4)$$

For the flat plate in continuum flow, then,

$$\overline{Nu} = 2Nu_x$$

Notice the heat transfer coefficient tends to increase toward the leading edge of the plate. Of course Eq. 2 holds only for x suffi-ciently large to assure continuum flow.

2.1.2. Turbulent flow over a flat plate

When the Reynolds number based on the distance from the leading edge has reached the critical value (approximately 3×10^5), the flow in the boundary layer becomes turbulent. The Nusselt number based on the average heat transfer coefficient for turbulent flow over the entire heated plate is given by [3]

$$\overline{Nu}_x = 0.037 \left(Re_x\right)^{0.8} (Pr)^{1/3} \qquad (5)$$

In reality a certain part of the boundary layer near the leading edge is always laminar. Integration must then be carried out in two separate steps, over the laminar part and over the turbulent part. However, assuming that the turbulent boundary layer starts right on the leading edge, integration yields [89]

- 5 -

$$\overline{Nu}_x = 0.037 \ (Pr)^{1/3} \left[(Re)^{0.8} - 23,100 \right] \qquad (6)$$

for critical Reynolds number 5×10^5, and

$$\overline{Nu}_x = 0.037 \ (Pr)^{1/3} \left[(Re)^{0.8} - 4,200 \right] \qquad (7)$$

for critical Reynolds number 10^5.

2.2. Cylinder

A boundary layer builds up on the forward side of the cylinder in the flow. This boundary layer is always laminar near the stagnation point [6]. If the cylinder is heated, a thermal boundary layer exists in the same way. In the immediate proximity of the stagnation point, the velocity outside the boundary layer increases linearly with the distance from the stagnation point as measured along the body surface. This is expressed by $u_s = cx$. The heat transfer in this region for cylindrical bodies with constant surface temperature in a flow normal to their axes was determined theoretically by Squire [3,4]. This calculation yields the local Nusselt number,

$$Nu_x = B \left(\frac{u_s x}{\nu} \right)^{1/2} \qquad (8)$$

where u_s is the free stream velocity and B is a constant tabulated as follows:

Pr	.7	.8	1.0	5.	10.
B	.496	.523	.570	1.043	1.344

- 6 -

From Eq. 8, the local heat transfer coefficient yields

$$h = Bk \left(\frac{u_s}{\nu x}\right)^{1/2} \tag{8.a}$$

where k is thermal conductivity.

For potential flow around a cylinder with circular cross sec-
tion, the velocity u_s outside the boundary layer is, according to
potential theory [3,4],

$$u_s = 2u_o \sin\left(\frac{2x}{d}\right) \tag{9}$$

where

u_s = velocity outside the boundary layer

$x = \theta \frac{d}{2}$ = the distance along the surface from the stagnation

point

d = the diameter of the cylinder

and

θ = angle of the point we are considering measured from the
stagnation point (radian)

In the neighborhood of the stagnation point, the "sine" can be replaced
by the angle. This gives

$$u_s = 4u_o \left(\frac{x}{d}\right) \tag{10}$$

and the local heat transfer in the neighborhood of the stagnation point
becomes

$$h = 2Bk\left(\frac{u_o}{\nu d}\right)^{1/2} \tag{11}$$

In the dimensionless form,

$$Nu_d = \frac{hd}{k}$$

$$= 2B\left(\frac{u_o d}{\nu}\right)^{1/2}$$

$$= 2B\left(Re_d\right)^{1/2} \tag{12}$$

where Nu_d and Re_d are based on free stream velocity and diameter.

The local heat transfer coefficient along the surface of a cylindrical body at a great distance from the stagnation point can be calculated from the integral energy equation [5, 6]:

$$\frac{d}{dx}\int_0^\ell (t_\infty - T)\,udy = \alpha\left(\frac{dT}{dy}\right)_\omega \tag{13}$$

where

T_∞ = free stream temperature

α = $k/\rho Cp$ = thermal diffusivity

and

subscript ω refers to wall.

Methods for such calculations have been developed by many investigators [3,7]. Usually the distance (x) from the stagnation point is divided by the greatest diameter of the cylinder (its major axis L) to make angle $\theta = s/L$ a parameter. In all laminar boundary layers the Nusselt number increases with the square root of the Reynolds number.

The flow around cylindrical and spherical bodies separates from the surface at about $\pi/2$ (varies from laminar to turbulent flow), and determination of the heat transfer coefficient for the separated part must consider the effect of separation.

The total heat flow from or to a tube, or the average heat-transfer coefficient around the circumference, is of interest. Hilpert [8] made accurate measurements of this average value for air flow as shown in Fig. 1. Nusselt and Reynolds numbers are calculated with the tube
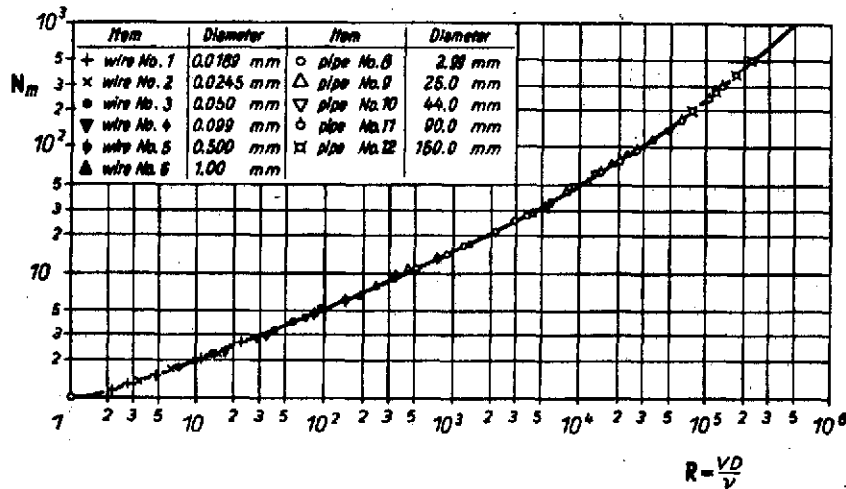
Fig. 1. Average film heat-transfer coefficient on a cylinder in flow of air normal to its axis. [6]

diameter as the reference length and with the free stream velocity as the reference velocity. From Fig. 1 and from the results of other experiments, especially at low Reynolds numbers, it can be seen that in various ranges of the Reynolds number, the Nusselt number can be presented in the form [3]

$$\overline{\mathrm{Nu}}_d = 0.43 + C\left(\mathrm{Re}_d\right)^m \tag{14}$$

- 9 -

The numerical values for the constants C and m are tabulated below [3]:

Re_d	C	m
1-4,000	0.48	0.50
4,000-40,000	0.174	0.618
40,000-400,000	0.0239	0.805

It should be noted that a high turbulent level in the approaching stream increases not only the average heat transfer coefficient, but also the local heat transfer on the upstream part of the cylinder circumference which is covered by laminar boundary layer. Increases in Nu_d up to 25 percent have been measured for turbulent levels up to 7 percent. (This is, however, of no concern in the upper atmosphere since the turbulence level of the free stream is very low due to the absence of the turbulence initiating factors.)

2.3. Sphere

Heat transfer at the surface of a sphere is determined by the flow conditions. Flow around a sphere resembles that around a circular cylinder. A laminar boundary layer covers the upstream portion of the sphere, and separates from the side of the sphere creating an irregularly fluctuating flow condition along the downstream portion. On the side of the sphere, the boundary layer may become turbulent at large Reynolds numbers, influencing the location of the flow separation.

The average heat-transfer coefficient for a sphere cannot be obtained by calculation since it is not possible yet to calculate the

heat transfer in the separated flow region on the downstream part of the sphere. The following relation was proposed by Grigull [9] from experiment:

$$\overline{Nu}_d = 0.37 \left(Re_d\right)^{0.6} (Pr)^{1/3} \qquad (15)$$

for a range $20 < Re_d < 150,000$. For small Reynolds numbers, the following relation was proposed [9]:

$$\overline{Nu}_d = 2 + 0.37 \left(Re_d\right)^{0.6} (Pr)^{1/3} \qquad (16)$$

Equation 16 describes the actual condition well, because as $Re_d \rightarrow 0$, this equation yields $Nu_d = 2$, which is the value for heat transfer by pure conduction.

3. Free Molecule Regime

3.1. Introduction

Free molecule flow is defined as the flow obtained in the limit when the Knudsen number becomes large. In that case, the Boltzmann equation takes the form [1, 10]

$$\frac{df}{dt} = \frac{\partial f}{\partial t} + \vec{\xi} \cdot \frac{\partial f}{\partial x} + \frac{\vec{F}}{m} \cdot \frac{\partial f}{\partial \xi} = 0 \qquad (17)$$

where

f = velocity distribution function

$\vec{\xi}$ = acceleration vector, $\vec{\xi} = d\vec{x}(t)/dt$

$\vec{F}$ = force vector, $\vec{F} = m \, d^2 \vec{x}/dt^2$

In such flows, the interaction of the molecules with the wall

- 11 -

plays a major role, while the collisions of the molecules among themselves may be neglected. A gas in which the molecules do not collide is called a Knudsen gas. For a given characteristic dimension of the flow, Knudsen gas may be represented as a gas in which the density and the diameter of the molecules tends to zero. Then the mean free path tends to infinity. The general solution of Eq. 17 in the absence of external forces has the form

$$f(t,\vec{\chi},\vec{\xi}) = f\left(t_o,\vec{x} - \vec{\xi}\left(t - t_o\right),\vec{\xi}\right) \qquad (18)$$

with the initial conditions,

$$\vec{x}\left(t_o\right) = \vec{\chi}_o, \ \vec{\xi}\left(t_o\right) = \vec{\xi}_o$$

With large Knudsen number, the heat conducted in unit time from unit area may be expressed approximately by Knudsen's formula [10]

$$q_{FM} = \frac{Q_{FM}}{A}$$

$$= \left[\frac{1}{\alpha_1} + (R^*)^b\left(\frac{1}{\alpha_2} - 1\right)\right]^{-1} \frac{P\left(C_y + \tilde{R}/2\right)}{(2\pi\tilde{M}\tilde{R}T)^{1/2}} \left(T_1 - T_2\right) \qquad (19)$$

where

   . $R^* = R_1/R_2$

   b (constant) = 0 for parallel plates

                = 1 for concentric cylinders

                = 2 for concentric spheres

   P = the pressure of a Maxwellian gas at the density at a temperature T

- 12 -

$T = \left(T_1 + T_2\right)/2$ for small temperature differences

$\tilde{M}$ = molecular weight of the gas

$\tilde{R}$ = molecular gas constant

C_y = molecular heat capacity at constant volume

The above equation is based on the assumption of diffuse reflection at the surface, where the tangential and normal momentum accommodation coefficients are equal to one. For parallel plates, Sparrow and Kinney [11] derived an expression for these accommodation coefficients. In the case of the parallel plate geometry, the approximate characteristic length is the separation between the plates L. For concentric cylinders and spheres, the choice of the characteristic length is not obvious. But Wachman [12] argues that the important characteristic length is the inner radius R_1. This is supported by many investigators [13, 14, 15]. The characteristic length is of great interest, because it is needed in defining the Knudsen numbers and Reynolds numbers accurately.

In order to determine the heat transfer to a body in a rarefied gas, it is necessary to know the flux of energy and momentum carried by the molecules impinging on and reemitted from the surface. The thermal accommodation coefficient is defined by [1]

$$\alpha = \frac{E_{in} - E_{re}}{E_{in} - E_w} \qquad (20)$$

E_{in} and E_{re} are the incident and reflected energy fluxes from the surface, and E_w is the energy flux which the molecular stream carries away from the surface at the surface temperature T_w. The thermal accommodation coefficient may vary between 1 (complete accommodation, diffuse

reemission) and 0 (specular reemission). In experiments it is difficult
to ensure that the surface is free of contaminants and, therefore, re-
ported values of the coefficient range from 0.01 to nearly 1.0, depend-
ing on the condition of the surface. The surfaces most commonly used
for engineering purposes are not clean, but contain some contaminants.
For such surfaces the accommodation coefficient may vary between 0.8
and 0.98.

The momentum accommodation coefficient must be defined to predict
the energy transport properly. Schaaf and Chambre [1] suggested the
following tangential and normal accommodation coefficients which are
similar to the thermal accommodation coefficient

$$\delta = \frac{\tau_{in} - \tau_{re}}{\tau_{in} - \tau_{w}} \qquad (21)$$

and

$$\delta' = \frac{P_{in} - P_{re}}{P_{in} - P_{w}} \qquad (21.a)$$

τ and P are tangential and normal components of the momentum. The
subscripts have the same meaning as in the thermal accommodation
coefficient. For completely diffuse reflection $\delta = \delta' = 1$, and for
completely specular reflection $\delta = \delta' = 0$. For common engineering
surfaces δ is in the range 0.8 to 1.

3.2. Review of Theory

3.2.1. Oppenheim theory

In the free molecular regime, the density is so low that the

structure of the gas cannot be considered continuous. Therefore, the molecular structure is taken into consideration. This suggests that heat transfer between an object and a rarefied gas stream in this regime can be calculated entirely from the fundamental motions of the kinetic theory of gases. Oppenheim [16] was successful in developing a theory for predicting the heat transfer coefficient and thermal recovery factor. Oppenheim gave the following relation for Stanton number:

$$St = \frac{h}{\rho C_p u} = \frac{\gamma + 1}{2\gamma} \alpha \ (\overline{G} + \overline{F}) \tag{22}$$

where

α = thermal accommodation coefficient

$$\overline{G} = \frac{1}{A} \int_A \frac{e^{-\phi^2}}{2s\sqrt{\pi}} \, dA \tag{22.a}$$

$$\overline{F} = \frac{1}{A} \int_A \frac{\phi(1 + erf\phi)}{2s} \, dA \tag{22.b}$$

and

A = surface area

ϕ = $u_\eta/\overline{V}_m$ = $s \sin \theta$ (dimensionless)

u_η = component of mass flow velocity u normal to the wall

$\overline{V}$ = most probable molecular velocity (m/sec)

s = $u/\overline{V}_m$ = $\gamma M/2$ = speed ratio (dimensionless)

M = Mach number

Oppenheim calculated Stanton number for various geometrical shapes and presented the results in the form of plots as shown in Fig. 2. He also presented an approximate expansion of Eq. 17 for various shapes,
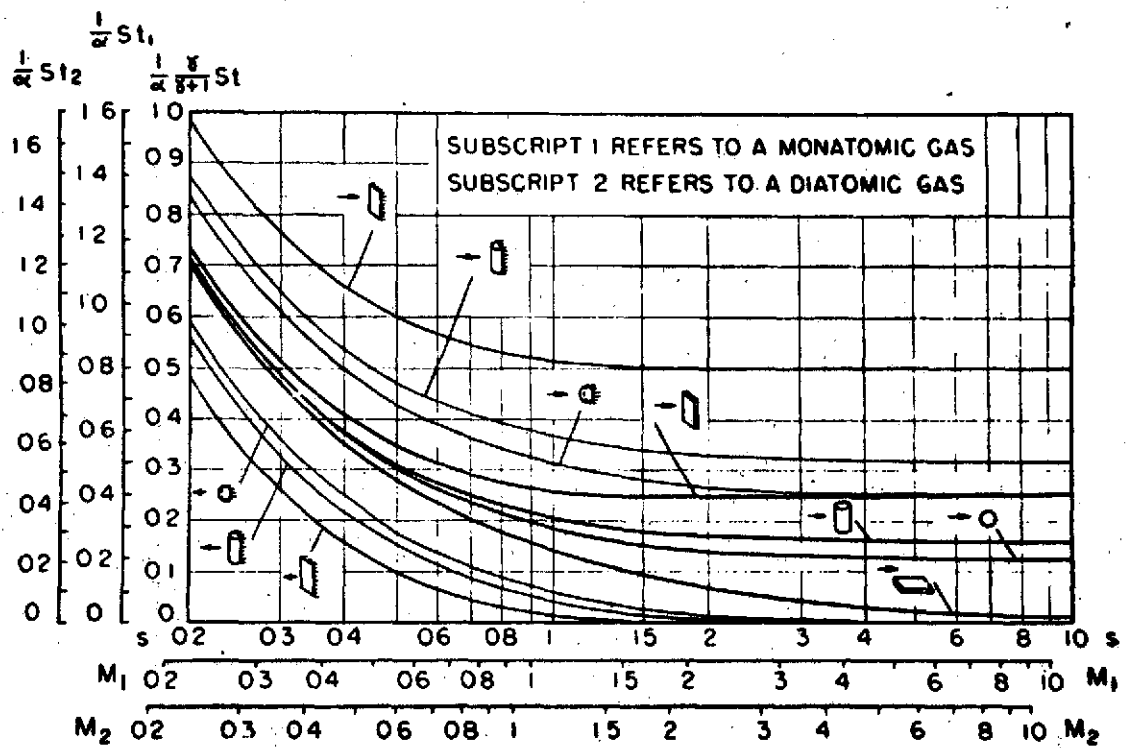
- 15 -

Fig. 2. Heat transfer from a flat plate, a sphere, and a transverse
circular cylinder in a free molecule flow. [16]

and pointed out that the flat plate results could be applied to any surface making a constant angle θ with the flow. Thus

$$St_\theta = St_n(\phi) \sin \theta \qquad (23)$$

where the subscript n indicates a flat plate normal to the flow, and

$$\phi = s \sin \theta \qquad (23.a)$$

Therefore, the flat plate results apply to wedges and cones in comparison with flat plates at an incident angle of θ with the flow, where the angle of incidence of the plate corresponds to half the opening angle of the wedge or cone. Conditions on the flat plate with zero incident angle correspond to those occurring on a cylinder of any cross-sectional shape in axial flow. He proposed the following equations for Nusselt number for various shapes:

For plate

$$Nu_{FM} = RePr \frac{\gamma + 1}{\gamma} \frac{\alpha}{4s\sqrt{\pi}}, \quad s = \sqrt{\frac{\gamma}{2}} M \qquad (24)$$

For right circular cylinder in a flow perpendicular to its axis

$$Nu_{FM} = RePr \frac{\gamma + 1}{\gamma} \alpha \frac{1}{4\sqrt{\pi}} e^{-\frac{s^2}{2}} \left\{ \frac{1}{s} I_o\left(\frac{s^2}{2}\right) + s \left[I_o\left(\frac{s^2}{2}\right) + I_1\left(\frac{s^2}{2}\right) \right] \right\} \qquad (25)$$

For sphere

$$Nu_{FM} = RePr \frac{\gamma + 1}{\gamma} \frac{\alpha}{8} \left[1 + \frac{1}{s} ierfc(s) + \frac{1}{2s^2} erf(s) \right] \qquad (26)$$

- 17 -

where

$I_0(s)$ = modified Bessel function of first kind and zeroth order,

$$\frac{1}{\pi} \int_0^\pi e^{-s \cos \theta} d\theta \quad \text{(dimensionless)}$$

$I_1(s)$ = modified Bessel function of first kind and first order,

$$-\frac{1}{\pi} \int_0^\pi e^{-s \cos \theta} \cos \phi \, d\theta \quad \text{(dimensionless)}$$

$ierfc(s)$ = integral of complementary error function $\int_0^\infty (1 - erfx)dx$

(dimensionless)

$erf(s)$ = error function

$$= \frac{2}{\sqrt{\pi}} \int_0^s e^{-x^2} dx \quad \text{(dimensionless)}$$

Comparing the Oppenheim theory with the experimental data reported in reference 17 yields a maximum error of about 7 percent, due mainly to the variation of the accommodation factor.

3.2.2. Others

Oppenheim theory was based on the assumption that only convective heat transfer takes place. Shidlovskiy [20] made some correction to the Oppenheim theory by considering radiation effects in addition to the convective effects. Radiation plays a substantial role in the general ensemble of the thermal process under certain conditions. The general heat loss can be expressed by

$$q = q_{conv} + \varepsilon\left(\sigma T_\omega^4 - J_o\right) \tag{27}$$

where

ε = emissivity of the body

σ = Stefan-Boltzmann constant

J_o = the radiation flow from the outside source

q_{conv} = heat loss due to convective heat transfer

$$= \frac{\alpha P_\infty}{\sqrt{2\pi}}(RT_\infty)^{3/2}\left\{\frac{1}{2}e^{s^2}\sin^2\theta + \left(e^{-s^2\sin^2\theta} - \sqrt{\pi}\,s\,\sin\theta\right.\right.$$

$$\left.\left. \times\left[1 + \mathrm{erf}(s\,\sin\theta)\right]\right)\left[\frac{\gamma+1}{2(\gamma-1)}\frac{T_\omega}{T_\infty} - s^2 - \frac{\gamma}{\gamma-1}\right]\right\} \tag{27.a}$$

For circular cylinder in a flow perpendicular to its axis, Atassi and Brun [21] deduced another practical equation for the free molecule, subsonic region.

Let the convective heat transfer rate be

$$q = St\ Cp\ \rho_\infty u_\infty\left(T_\omega - T_{a\omega}\right) \tag{28}$$

where

St = Stanton number

Cp = specific heat at constant pressure

ρ_∞ = free molecular density

u_∞ = free stream velocity

$T_{a\omega}$ = adiabatic cylinder wall temperature

Then, considering adiabatic wall temperature, another form of Stanton number will be possible.

$$q = St'Cp\rho_\infty u_\infty \left(T_\omega - T_\infty \right) \tag{29}$$

From Eqs. 23 and 23.a,

$$St' = St \; \frac{T_\omega - T_{a\omega}}{T_\omega - T_\infty} \tag{30}$$

By Eq. 24, we can evaluate St' which is a function of T_ω, and is also weakly dependent upon the mean overheat C_m, where

$$C_m = \left(\frac{T_{\omega i} + T_{\omega j}}{2} - T_{a\omega} \right) \Big/ T_{a\omega} \tag{31}$$

where

$T_{a\omega}$ = adiabatic cylinder wall temperature

T_ω = cylinder temperature

C = overheat, $\left(T_\omega - T_{a\omega} \right) \big/ T_{a\omega}$
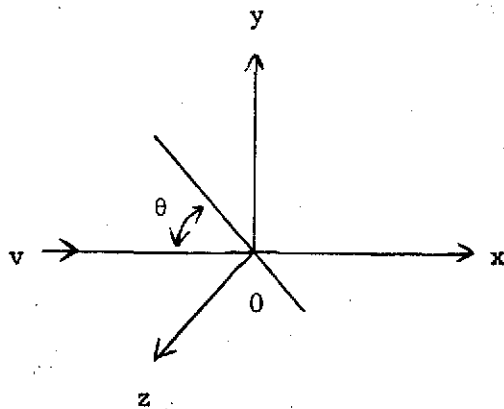
C_m = mean overheat

Fig. 3. Coordinates of a body in a free molecule flow [22].

In this case, Kogan [22] solved the Maxwell velocity distribution function as

$$f_\infty = n_\infty \left(\frac{h_\infty}{\pi}\right)^{3/2} \exp\left\{-h_\infty(\zeta - v)^2\right\} \tag{32}$$

where

$$h_\infty = \frac{m}{2KT_\infty}$$

n_∞ = number density

For hypersonic free-molecule flow, the Stanton number becomes [22],

$$St = \frac{2\gamma}{\gamma + 1} \frac{Q}{A\rho_\infty v \left(T_{eq} - T_\omega\right)\alpha} \tag{33}$$

where

α = average accommodation coefficient

A = area of the body

v = free stream velocity

T_{eq} = equilibrium temperature

T_ω = wall temperature of the body

Q = average heat transfer rate = $\frac{1}{A} \int_A q\, dA$

Equation 33 is similar in form to Oppenheim's Eq. 22. Figures 4 and 5 show the results of the calculation for drag coefficient and Stanton number, respectively. In calculating the drag coefficient, the cylinder and sphere are referred to a normal area section, while the plate is referred to the area of one side. It is assumed that $T_t = T_\omega = T_\infty$, or $\alpha = 1$.
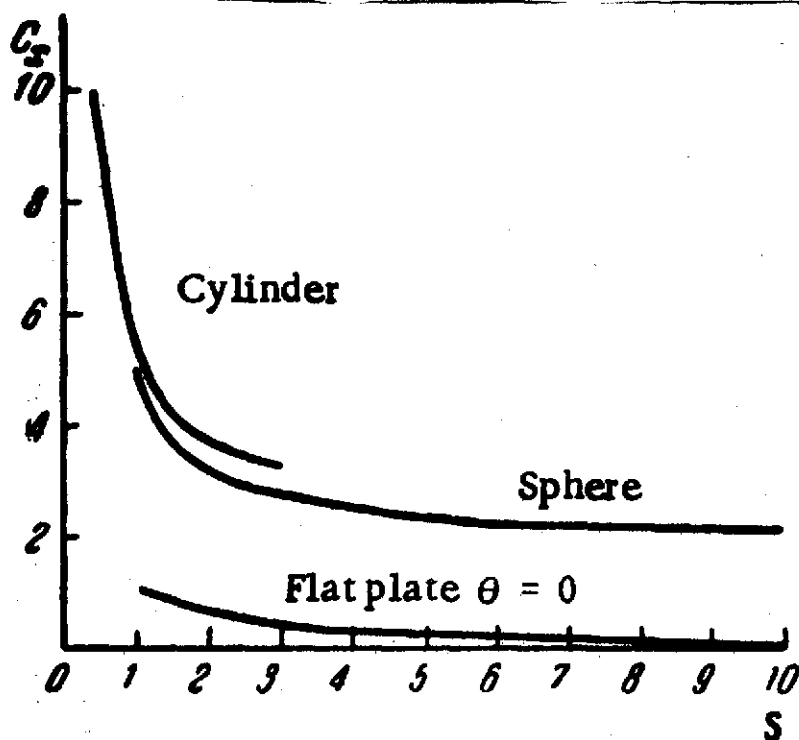
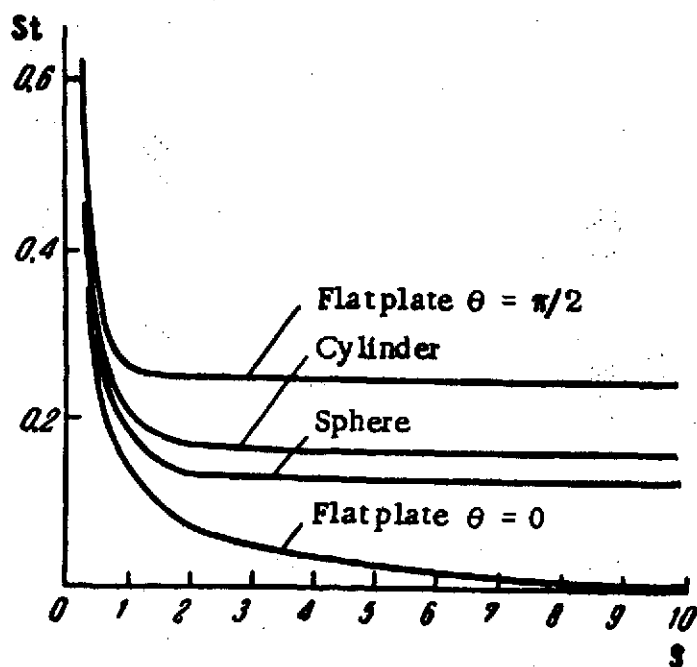Fig. 4. Free molecule flow past convective bodies [22].

Fig. 5. Free molecule flow past convective bodies [17].

In addition to the heat transmitted to the surface by the incident molecules, the surface may receive heat from sources in the body, from heat conduction in the body, and from radiation. Usually $T_\omega/T_\infty \le 1$; i.e., the body may be considered cold. In general, the calculation reduces to very laborious quadratures, especially if one does not make the assumption that T_r is constant over the body surface.

Schaff [1] and Hayes [2] derived the following expression for convective heat transfer per unit time to a unit surface (dA) of a convex body immersed in the steady, uniform, free molecule flow of a perfect gas.

$$dQ_{FM} = \alpha\rho_\infty \tilde{R}T_\infty \sqrt{\frac{\tilde{R}T_\infty}{2\pi}} \left(\left[s^2 + \frac{\gamma}{\gamma + 1} - \frac{\gamma + 1}{2(\gamma - 1)} \frac{T_\omega}{T_\infty} \right] \left[e^{-\phi^2} + \phi\sqrt{\pi}\,(1 + \mathrm{erf}\phi) \right] \right.$$
$$\left. - \frac{e^{-\phi^2}}{2} \right)\ dA \tag{34}$$

$\phi = s \sin \theta$, and θ is the local angle of attack as shown in Fig. 3. T_ω is the wall temperature. The subscript ∞ refers to free stream conditions. s is the speed ratio defined in Eq. 24, u_∞ is the free stream velocity.

At very large Mach number, Hayes and Probstein [2, 48] convert Eq. 34 to

$$dQ_{FM} = \frac{1}{2} \alpha\rho_\infty u_\infty^3 \sin \theta \left(1 - \frac{1}{2} \frac{\gamma + 1}{\gamma - 1} \frac{T_\omega}{T_\infty} \frac{1}{s^2} \right) dA \tag{35}$$

From Eq. 35, the adiabatic recovery temperature can be calculated as

$$\frac{T_r}{T_\infty} = \left[2(\gamma - 1)/(\gamma + 1)\right] s^2 \qquad (36)$$

Therefore, if heat transfer occurs due to convection only, T_r is independent of both α and θ. For high values of s the stagnation temperature of the flow is given by [1,2]

$$T_o = T_\infty \left(1 + \frac{\gamma - 1}{\gamma} s^2\right) \approx T_\infty \left(\frac{\gamma - 1}{\gamma} s^2\right) \qquad (37)$$

From Eqs. 36 and 37, Stalder, Goodwin, and Craeger [17] found that in high speed free molecule flow, the recovery temperature is higher than the free stream stagnation temperature. When s sin θ is large compared to both unity and $\sqrt{T_\omega/T_\infty}$ (highly cooled surface), Eq. 35 becomes

$$dQ_{FM} = (1/2) \alpha \rho_\infty u_\infty^3 \sin \theta \, dA \qquad (38)$$

Equations 35 and 38 show the Mach number independence principle [16,17], namely that in high speed rarefied flows, the heat transfer depends only on u_∞, ρ_∞, T_ω and α.

Using Eq. 34, heat transfer rates can be calculated in terms of the modified recovery factor and modified Stanton number.

$$r' \equiv r \frac{\gamma + 1}{\gamma} = \frac{T_r - T_\infty}{T_o - T_\infty} \frac{\gamma + 1}{\gamma} \qquad (39)$$

$$St' \equiv St \frac{\gamma}{\gamma + 1} = \frac{Q}{\alpha A \rho_\infty u_\infty Cp \left(T_r - T_\omega\right)} \frac{\gamma}{\gamma + 1} \qquad (40)$$

which is similar to Eq. 33.

For a flat plate at an angle of attack θ (Fig. 4) [1],

$$r' = \left(\frac{1}{s^2}\right) \left\{ 2s^2 + 1 - \left[1 + \sqrt{\pi}\ (N + \text{erf}\phi)\ e^{\phi^2} \right]^{-1} \right\} \tag{41}$$

$$St' = \left[\frac{1}{4\sqrt{\pi}s} \right] \left[e^{-\psi^2} + \sqrt{\pi}\phi (N + \text{erf}\phi) \right] \tag{42}$$

where

$$\phi = s \sin\theta$$

When the front and rear surfaces are isolated, A is the surface of one side only and $N = 1$. For the rear surface θ is replaced by $-\theta$. When both front and rear surfaces are in thermal contact, then A is the total surface area and $N = 0$.

For a circular cylinder of surface area A at an angle of attack θ (Fig. 4), Talbot [21] gives

$$r' = 2 + \sin^2\beta \left[I_0\left(\frac{\phi^2}{2}\right) + I_1\left(\frac{\phi^2}{2}\right) \right] / \left[\left(1 + \phi^2\right) I_0\left(\frac{\phi^2}{2}\right) + \phi^2 I_1\left(\frac{\phi^2}{2}\right) \right] \tag{43}$$

$$St' = \left[\sin\theta/(4\sqrt{\pi}) \right] \left\{ \left[\frac{1}{\phi} + \phi \right] I_0\left(\frac{\phi^2}{2}\right) + \psi I_1\left(\frac{\phi^2}{2}\right) \right\} e^{-\phi^2/2} \tag{44}$$

For a sphere with surface area A, Schaaf and Chambre [1] reported the result of Sauer [24]

$$r' = \frac{\left(2s^2 + 1\right)\left[1 + (1/s)\text{ierfs} \right] + \left(2s^2 - 1\right)(\text{erfs})/\left(2s^2\right)}{s^2\left[1 + (1/s)\text{ierfs} \right] + (\text{erfs})/\left(2s^2\right)} \tag{45}$$

$$St' = \left[1/\left(8s^2\right) \right] \left[s^2 + s\,\text{ierfcs} + (\text{erfs})/2 \right] \tag{46}$$

where the notations are the same as those in Eqs. 25 and 26.

The above results must be modified for a nonuniform gas in which the distribution function is different from the Maxwellian distribution because of the presence of viscous stresses and heat flow [25], and as indicated the results are applied for high Mach numbers. Expressions for heat transfer to cylinders and spheres for the free molecule flow of a nonuniform gas were derived by Bell and Schaaf [26] and Touryan and Maise [27]. Combined radiative and convective heat transfer for large Mach numbers were handled by Stalder and Jukoff [28], Stalder, Goodwin and Craeger [17], and Abarbanel [29]. Numerical solutions for flat plates are presented in Eckert [7], which includes the effect of solar radiation on the surface temperature of bodies in high altitude flight. Abarbanel [28] developed general results for the surface temperature of bodies in free molecule flow when both convective and radiative transport are significant. The adiabatic recovery temperature of a surface element with local angle of attack θ for high speed flows $\left(s^2 \gg 1, s \sin \theta > 1\right)$ as derived by Abarbanel [29] is

$$T_r = \left\{ \left(2s^2 + \frac{5 - 3\gamma}{\gamma - 1}\right) \alpha \frac{\rho_\infty}{m}(kT_\infty)^{3/2} \left[\frac{e^{-\phi^2}}{\sqrt{4\pi}} + \frac{\phi}{2}(1 + \text{erf}\phi)\right] \Big/ 4\sqrt{2m} \, e\delta \right\}^{1/4}$$

(47)

for convex surface to the flow. Where k is the Boltzmann constant, m is the molecular mass, e is the emissivity and absorptivity of the surface, and δ is the Stefan-Boltzmann constant. Concave surfaces in free molecule flow were investigated by Sparrow [30], Schamberg [31], and Chanine [32].

3.3. Analysis of Experimental Results

3.3.1. Flat plate

Experiments for the heat transfer coefficients of free molecule flow past a flat plate at zero angle of attack have been studied quite extensively in the supersonic and hypersonic range, but unfortunately little work has been done for the subsonic region. However, by empirical results, we can correlate the local Nusselt number, Nu_x (Re, M), and get a free molecule curve which is close to the free molecular theory curve. It is inevitable there exist some deviation between the two curves, say 7 percent maximum accuracy for Oppenheim theory [16].

However, the Oppenheim theory agrees very well with the experimental data. Interpolation of the theoretical values of continuum and free molecule flows by the law

$$Nu = \frac{1}{\dfrac{1}{Nu_c} + \dfrac{1}{Nu_{FM}}}$$

into the transition regime, yields values which are very close to experimental data in that regime.

3.3.2. Cylinder

Predictions by Stalder, Goodwin, and Creager [17] agree well with the experimental results of Vrebalobich [33], and Atassi and Brun [21] in the subsonic region. Vrebalobich [33] made a successful experimental work on the transition flow regime, between slip and near free molecule regime.

Atassi and Brun [21] found that for the subsonic region, the

dependence of the convection coefficient "h" upon Mach number is weaker in the free molecule flow than in continuum flow.

The theoretical curves [17] and the experimental data are compared for supersonic flow in Fig. 6. Close examination of this figure shows the departure in the free molecule regime and continuum regime from the transition regime.
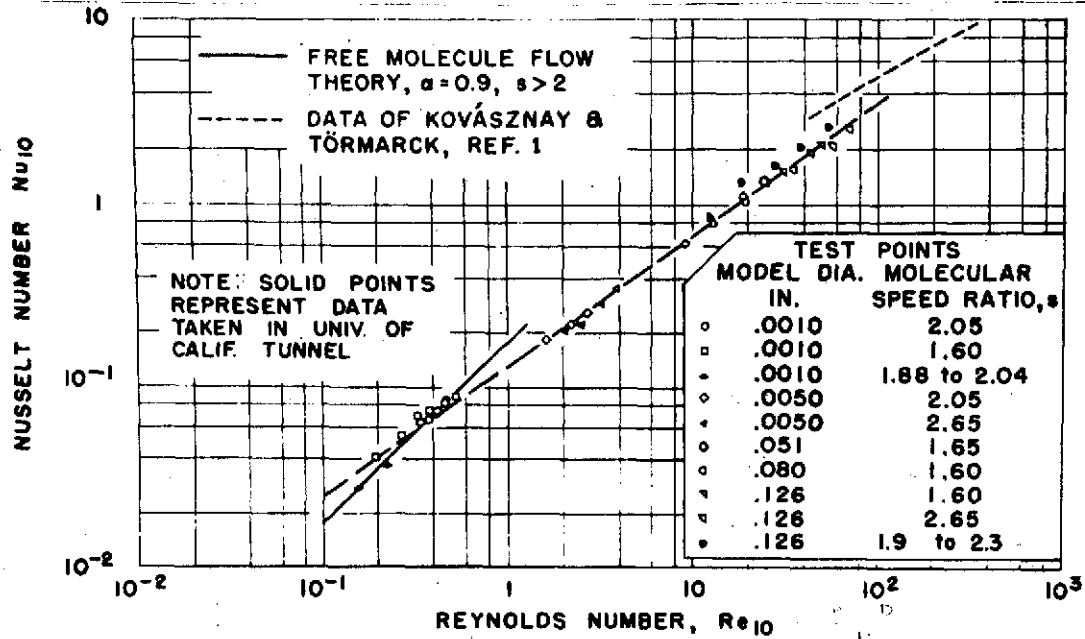

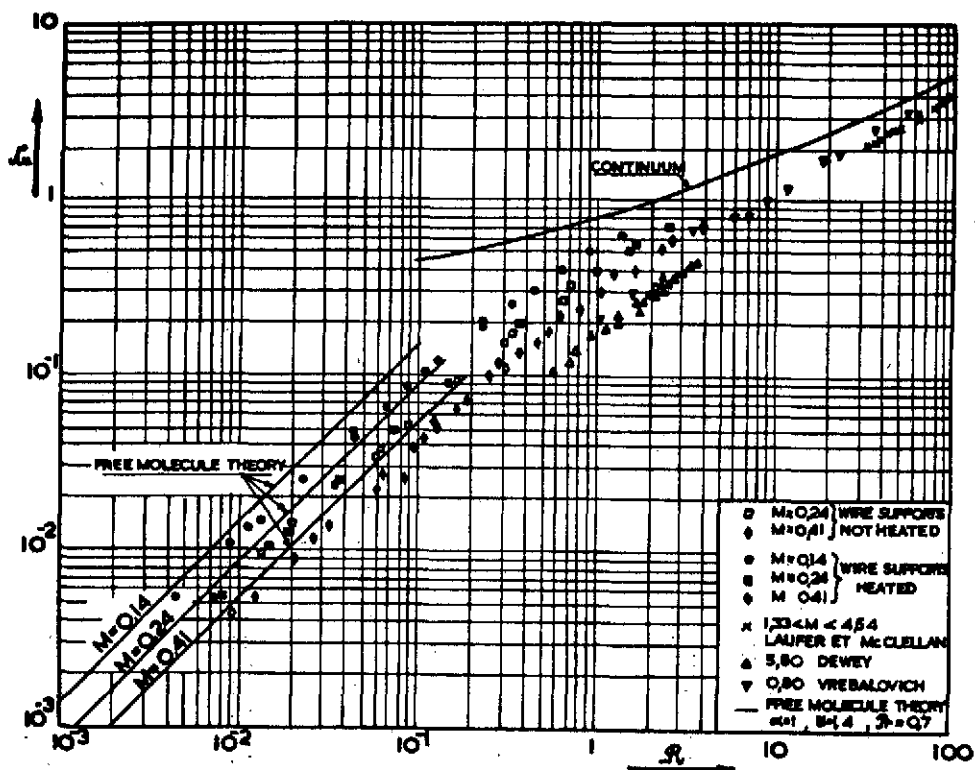Fig. 6. Convective heat transfer coefficients for transverse cylinders in supersonic flow. [17, 18, 19]

Fig. 7. Nusselt number versus Reynolds number in rarefied subsonic flow. [21]

3.3.3. Sphere

Very little experimental data exists for the sphere, especially for the free molecular flow regime. Therefore, in this regime the required data is determined by assuming that the free molecular flow theory applies [3], and by utilizing the experimental results from transition and slip flows.

Figure 8 supports the above argument. The general trend of the curve is very similar to that of the cylinder.
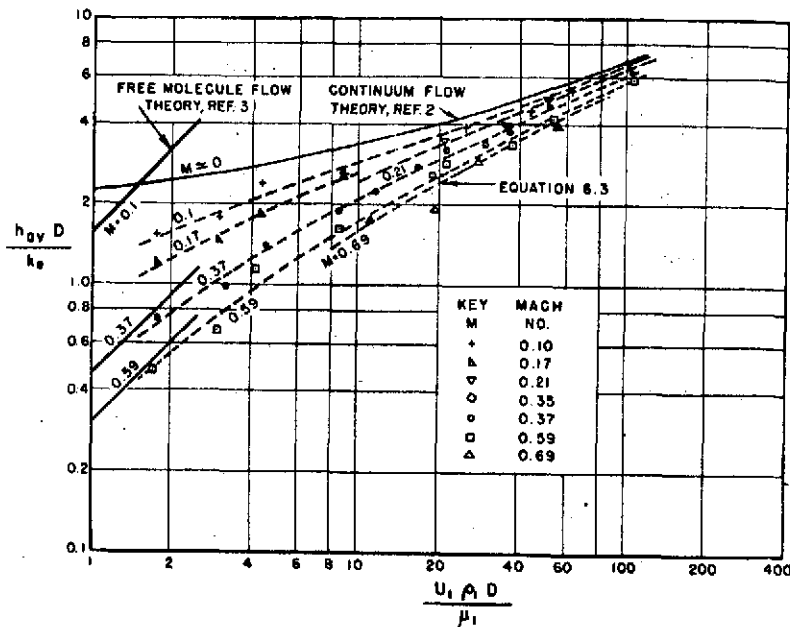
Fig. 8. Heat transfer coefficients for spheres in subsonic flow [43,93].

3.3.4. Generalization

From previous analysis, the theory which is closest to experimental data for subsonic flow is the Oppenheim theory. Many investigators [1,34] obtained very good experimental data for the near free molecular or transition regime, but not for the free molecular regime. Close examination of their empirical results reveals an important observation in the free molecule region. It confirms the prediction of kinetic theory in its present form with the momentum and energy flux of reemitted molecules estimated in terms of macroscopic and empirically determined accommodation coefficients. This indicates a significant collision rate in the gas surrounding a body, or enclosed within some walls. In free molecule regime the effects of momentum and energy transfer between the gas and the walls are largely reduced. The deviation from the free molecular values of the dependent variables occurs for Knudsen numbers ranging from about 5 to 15. So far, the reason for deviation from the free-molecular theory is not clear [34]. But this deviation can be fitted within expressions of the form, $Nu = Nu_f - A/k$, where A may depend on Mach number, temperature ratio, or geometry [34]. In subsonic free molecular flow, by the analogy of $Nu = Nu (Re, M)$, some useful analysis can be made by letting $M \to 0$ at fixed Reynolds number, without loss of qualitative information. This results in a correlation [34] which eliminates Mach number as a parameter in the transition or free molecule curves for all subsonic data.

Reasonable accuracy of $Nu (Re,M)$ in free molecule flow regime is still that of Oppenheim theory, in which the accuracy is within 7 percent compared to the experimental data [17, 34].

4. Transition and Slip Flow Regime

4.1. Introduction

4.1.1. Transition regime

A complete satisfactory formulation of the flow and energy equations to yield results on heat transfer and skin friction in the slip and transition regimes has not been sufficiently completed at the present time [1]. In the foregoing discussion, the case of free molecule flow was considered in which the effects of molecular encounters have been entirely neglected. With increasing density the effect of these collisions begins to be important and the low density part of the transition regime begins. Jaffé [35] derived a general formulation of this regime, employing a perturbation expansion solution of the Maxwell-Boltzmann equation in the inverse power of the molecular mean free path. The velocity distribution function f in the transition flow regime is assumed to be of the form [1, 30, 36]

$$f = f_o \left[1 + \frac{L}{\ell} \zeta_1 + \left(\frac{L}{\ell} \right)^2 \zeta_2 + \cdots \right]$$

where

f_o = Maxwellian equilibrium velocity distribution function

ℓ = characteristic length

L = typical macroscopic dimension

$\left(\frac{L}{\ell} \zeta_1 \right) < 1$ = dimensionless correction parameter

Many analytical calculations have been performed in this regime by Heineman [37], Keller [38], Wang-Chang and Uhlenbeck [39], Kryzwoblocki [40], Szymanski [41], and Lunc and Lubonski [42]. Very extensive

experiments in this regime were performed for spheres and cylinders
(wire) in subsonic flows by Kavanau [43], Vrebalovich [33], Takao [36],
and Atassi and Brun [21] for different thermal accommodation coefficients.
Results agree with the values obtained from the free molecule theory,
which predicts some deviation at the beginning and end of that regime
from the transition regime and continuum regime, respectively [34].

In order to eliminate the dependence of the results on the
thermal accommodation coefficient and on the Mach number [22], the data
of the above investigators [21, 36, 43, 44] were revised in Fig. 9 as
St/St_{FM} versus St_{FM}/St_{c}. St is the Stanton number calculated from the
data, St_{FM} is the limit of St as Reynolds number goes to zero, and St_{c}
is the limit of St as the Mach number goes to zero. This idea was
suggested by Sherman [34]. In supersonic flows, a shock wave arises
in the undisturbed uniform free stream flow from the disturbed region.
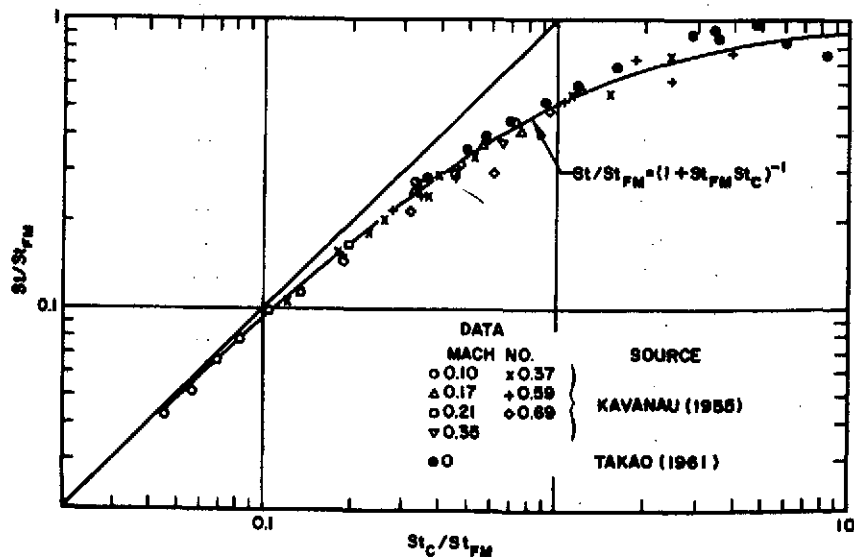
Fig. 9. Subsonic heat transfer from spheres [34].

Because of this the local mean free path around the object may be smaller than that of free stream. This affects the dimensions of the Knudsen number, boundary layer, viscous layer, merged layer, and collision rates, and eventually different heat transfer phenomena from the subsonic flow. Analyses of stagnation point and heat transfer phenomena were investigated by Rott and Lenard [45], Kemp [46], Herring [47], Probstein and Kemp [48], Ting [49], Van Dyke [50, 51, 52], Hickman and Giedt [53], Wittliff and Wilson [52], Potter and Mill [55], and Carden [56]. Details will not be discussed here, since this report is mainly concerned with the subsonic flow.

4.1.2. Slip flow regime

In the slip flow regime, there is a velocity slip at the wall [1, 22]. Therefore, the work done on the wall carries heat transfer which is different from that of free molecule flow. The gas density is slightly less than that characteristic of a completely continuum flow. In the slip flow, there are three important, but interrelated, parameters, the Mach number M, the Reynolds number Re, and the appropriate Knudsen number, M/Re or $M/\sqrt{Re}$ [1]. These parameters serve to indicate compressibility, viscosity, and rarefaction effects, respectively [1]. The Knudsen number is on the order of 0.01 to 0.1 [25]. The rarefaction effects are associated with very strong compressibility and viscous effects [1].

In general, the boundary layer will be laminar and thick for very low Reynolds number. Therefore, the boundary layer is not strictly applicable [22, 25]. Interaction effects between this thick viscous layer and an inviscid layer are expected [1]. The general effect of

the slip flow and temperature jump condition is to increase friction
and heat transfer, as described in Eq. 48.

$$q = K\left[\partial T/\partial y + \mu u_s(\partial u/\partial y)\right] \; y = 0 \qquad (48)$$

with slip velocity and temperature jump boundary conditions [1]

$$u(o) = \frac{2 - \alpha}{\sigma} \; \bar{\ell} \left(\frac{\partial u}{\partial y}\right)_o + \frac{3}{4} \frac{\mu}{\rho T} \left(\frac{\partial u}{\partial x}\right)_o$$

$$\qquad (49)$$

$$T(o) - T_\omega = \frac{2 - \alpha}{\alpha} \; \frac{2\gamma}{\gamma + 1} \; \frac{\bar{\ell}}{Pr} \left(\frac{\partial T}{\partial y}\right)_o$$

given by Kennard [10], where μ is viscosity and y is the coordinate
normal to the wall. Using Eq. 48, and various velocity and temperature
jump boundary conditions, Oman and Scheuing [57] obtained closed form
expressions for the recovery factor and for the heat transfer flow
over a flat plate.

Burnett [58] developed equations associated with the Maxwell
molecules, using the thirteen moment approach. These results are
presented in complete detail in references 59, 60, and 61. A method
of solution was suggested by many authors before Burnett [59, 62, 63,
64]. However, many difficulties arise in the actual problem, even
though the solution method is good for monoatomic Maxwell molecules
[1, 64]. For example, air is composed of diatomic nitrogen and oxygen
for the most part, and intricate boundary conditions make the problem
unresolvable. The order of the Burnett equations is higher than the
order of the Navier-Stokes equations, so that additional boundary
conditions are necessary [64]. Also, present experimental evidence

seems contrary to either the Burnett or thirteen moment equations, and although the linearized Boltzmann equation has been solved by Wang-Chang and Uhlenbeck [39], it was far from the practical case. Although it is very difficult to get an exact solution as a closed form, many authors [57, 58, 59, 65, 66, 67, 68] contributed valuable resolutions analytically and experimentally.

4.2. Flat Plate

The flat plate with zero angle of attack in a laminar flow was treated in terms of the Rayleigh problem of an impulsively started plate [1, 18]. The inertia and viscous terms in the Navier-Stokes equations can be simplified in this case [68, 70, 71, 72].

The heat transfer from the impulsively started plate was calculated [4, 73] from the energy equation. Neglecting heat conduction terms such as $\left(k \dfrac{\partial^2 T}{\partial x^2} \right)$ as being small in comparison with $\left(k \dfrac{\partial^2 T}{\partial y^2} \right)$, and also neglecting the convective terms in y, only the motion of the plate at constant velocity u in the x-direction is considered. The energy equation becomes

$$u \frac{\partial T}{\partial x} = \alpha \frac{\partial^2 T}{\partial x^2}$$ (50)

with boundary conditions

at $y = 0$, $x > 0$

$$T_{y=0} - T_\omega = \frac{2 - \alpha}{\alpha} \frac{2\gamma}{\gamma + 1} \frac{\lambda}{Pr} \left(\frac{\partial T}{\partial y} \right)_{y=0}$$ (51)

at x = 0, y > 0

$$T = T_f \ (= \text{free stream condition})$$

For accommodation coefficient $\alpha = 0.8$, and for $\gamma = 1.4$, the solution

of Eq. 50 becomes

$$St \ M = \frac{0.38}{x_2^2} \left(e^{x_2^2} \ \text{erfc} \ x_2 - 1 + \frac{2}{\sqrt{\pi}} \ x_2 \right) \tag{52}$$

where

$$x_2 = \sqrt{RePr/6.9M^2}$$

and

$$St = \frac{Nu}{RePr} = \frac{h}{u\rho Cp}$$

Unfortunately, at present there is no experimental data to

confirm Eq. 52; however, it is reported [3] that its accuracy is about

10 - 15 percent error. This estimation was based on the accuracy of

the skin friction relation which was developed for the flat plate in

the translation and slip regime using the same technique [3, 17, 34].

It should be pointed out here that Eq. 52 was developed essentially

for the slip flow regime and that its extension to the transition regime

implies the increase of its error in this regime.

Drake and Kane [73] solved the heat transfer from a flat plate

for the transition regime, neglecting dissipation terms and assuming

constant properties, but considering a surface temperature jump boundary

condition. Solving the energy equation through Laplace transform yields

$$\frac{h_x x}{k} = \frac{Pr}{\theta} \frac{x}{\ell} \exp\left(\frac{2.25}{\theta} \frac{Re_x Pr}{M^2}\right) \text{erfc} \frac{1.5}{\theta} \sqrt{\frac{Re_x Pr}{M}} \tag{53}$$

where

$$\theta = 1.996 \frac{(2 - \alpha)}{\alpha} \frac{\gamma}{\gamma + 1}$$

The average Nusselt number can be written from Eq. 53 by integrating along the plate length to x = L, remembering θ = 1.48, Pr = 0.72 for air.

$$\overline{Nu} \text{ average} = \frac{h_{av} L}{k}$$

$$= 2.25 \, M \left\{ \exp\left(\frac{Re_\ell}{1.35M^2}\right) \text{erfc} \sqrt{\frac{Re_\ell}{1.35M^2}} - 1 + \frac{2}{\sqrt{\pi}} \sqrt{\frac{Re_\ell}{1.35M^2}} \right\} \tag{54}$$

From Eq. 54, the average Nusselt number for the continuum regime where the Reynolds number is very large and Mach number is small can be predicted.

$$\overline{Nu} = 2.19 \sqrt{Re_\ell} \tag{55}$$

But actually, the constant is four times as large, compared to experimental results [73].

Accuracy of Eq. 54, compared with the results of experiments, is predicted within 20 percent by the analogy of the skin friction experimental data of the flat plate [34, 73].

Oman and Scheuing [57] obtained closed form expressions for the recovery factor and for the heat transfer in laminar slip flow over a flat plate.

4.3. Sphere

The problem of obtaining experimental results for heat transfer from a sphere in the slip and transition regimes is complicated by the fact that unless the sphere diameter is very small (0.001"), the Mach number must be large enough to establish the flow in the slip regime [43]. Ordinarily, this means that the flow is supersonic. In such a case, a shock wave exists in front of the sphere and the conditions behind this shock wave must be considered before any attempt can be made to calculate the heat transfer. Fortunately, in the rarefied subsonic flow at a very low density, such a shock wave is not present and, therefore, offers no real problem [3]. Kavanau [43] has developed an expression for the rarefaction correction to the continuum solution for heat transfer from spheres. His expression represents the experimental data to within 10 percent. Kavanau obtained the following relation for the average Nusselt number in the slip flow:

$$Nu_{av} = \frac{\overline{Nu}^{\,o}}{1 + 3.42 \left(\dfrac{M}{RePr}\right) \overline{Nu}^{\,o}} \tag{56}$$

where

$\overline{Nu}^{\,o}$ = average Nusselt number in the continuum region

M = Mach number

Re = Reynolds number

Pr = Prantdl number

Equation 56 can also be predicted from Oppenheim theory for the sphere in the near free molecule regime, which is very important to the calculation of heat transfer from the sphere in the transition regime. Drake and Kane [73] gave a solution for $\overline{Nu}^{\,o}$ as

$$\overline{Nu}^o = \frac{h_{av}D}{k}$$

$$= 2 + \frac{2}{\pi^2} \int_0^\infty \frac{\left(1 + e^{-\theta^2\pi}\right)\left(1 + \theta^4\right)^{-1} d\theta}{J_1^2\left(\alpha_1\theta\right) + Y_1^2\left(\alpha_1\theta\right) d\theta} \qquad (57)$$

where

D = diameter of sphere

$\alpha_1 = \sqrt{2RePr}$

and

$J_1\left(\alpha_1\theta\right)$ and $Y_1\left(\alpha_1\theta\right)$ are the Bessel function of the first order of the first kind and second kind, respectively.

Kavanau [43] obtained the average heat-transfer coefficients for spheres in a subsonic air stream for the slip flow regime in the range of Mach number $1.75 \leq Re < 124$. He also estimated the maximum uncertainty in the determination of the heat transfer coefficient to run as high as 25 percent. According to his paper, the error is mainly from the inaccurate value of Mach and Reynolds numbers, and the maximum relative errors of these quantities vary from 0.1 to 25 percent.

Drake and Backer [74] performed experiments on spheres in super-sonic flow. The Mach number range was $2.24 \leq M \leq 3.50$ and Reynolds number range was $16 \leq Re \leq 980$. They reported that the maximum error in calculating the total heat transfer coefficient might possibly be 7 to 8 percent, mainly due to the recording of instruments, such as the potentiometer at low temperature ($0.5°F$).

It should be noted here that Eq. 56 was derived by Kavanau [43] for spheres in a subsonic flow for the slip flow regime. However, Drake

and Backer [74] and Eckert [3] pointed out that Eq. 53 is applicable

for supersonic flow in the slip flow regime.

For the transition flow regime $\left(10^{-1} < Re < 10^2\right)$ there is not

enough experimental data for the low Reynolds number region, $Re > 10^{-1}$.

But for $1 < Re < 20$, the experimental data for various subsonic Mach

numbers are available from Kavanau's paper [43], and Eq. 56 predicts

the shapes of curves very precisely for subsonic Mach numbers. The

inaccuracy is as high as from 0.1 percent to 20 percent [43], due to

the inaccuracy of measuring Reynolds number and Mach number [43]. For

low Reynolds number, $Re < 1$, the free molecular flow theory by Sauer

[75] gave a good prediction which compares well to Eq. 56 in the

proximity of Reynolds number 1. Experimental data for this transition

flow regime are not available at this time.

Figure 9 was drawn out of Figs. 10 and 11 by Sherman [34]. This

figure implies the very important aspect of heat transfer coefficient

in the transition and slip regime by correlating three quantities; (1)

$F(M, Re)$, the measured quantity in such dimensionless form that it

becomes independent of Re in the free molecule limit, (2) $F_{FM}(M)$, the

limit of F as $Re \rightarrow 0$, which is generally available from theory, and (3)

$F_c(Re)$, the limit of F as $M \rightarrow 0$, which may be available either from

theory or from experiments in viscous liquids. The transition curve

approaches this line asymptotically in the continuum limit, and approaches

this line asymptotically in the free molecule limit (Fig. 11). Within

the experimental accuracy claimed for the data of Fig. 10 (the maximum

error for the average overall convection heat transfer coefficient, h_c,

is possibly 25 percent [43], the elimination of apparent Mach number
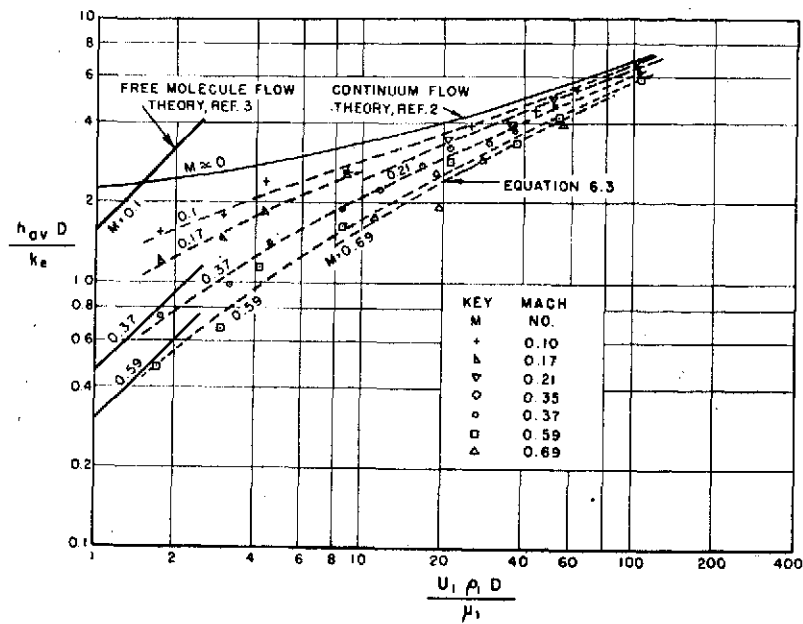
Fig. 10. Average heat-transfer coefficients for spheres in subsonic flow to rarefied air [43].
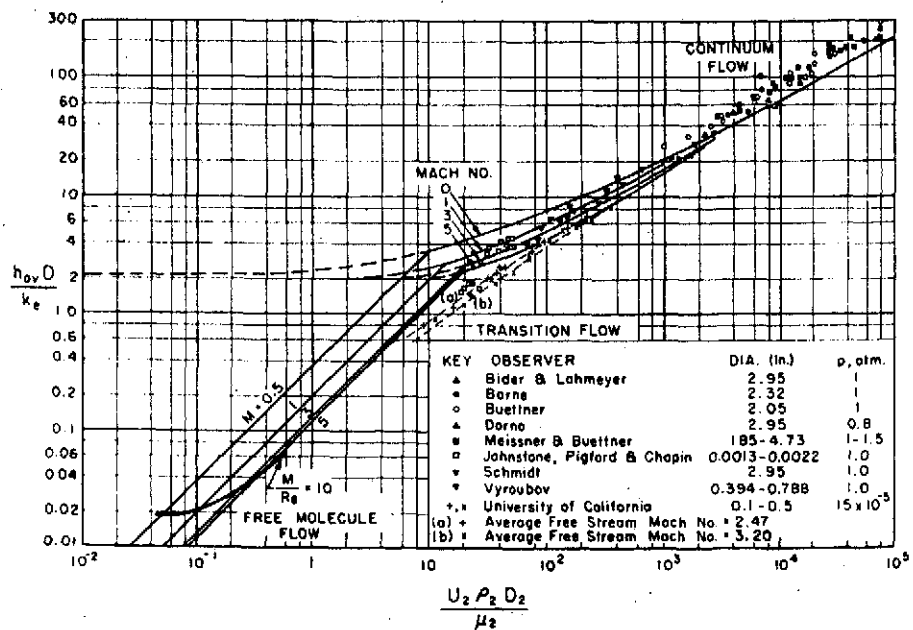
Fig. 11. Heat transfer from spheres [74].

dependence is perfect for the heat transfer coefficient of a sphere if we examine Fig. 10 carefully.

This is obviously true directly from Eq. 56. Rearranging Eq. 56,

$$Nu = \frac{1}{\frac{1}{Nu_c} + \frac{1}{Nu_{FM}}} \tag{58}$$

or

$$\frac{Nu}{Nu_{FM}} = \frac{1}{1 + \frac{Nu_{FM}}{Nu_c}} = \left(1 + \frac{Nu_{FM}}{Nu_c}\right)^{-1} \tag{59}$$

Therefore, in log-log scale of Nu_c/Nu_{FM} versus Nu/Nu_{FM}, Eq. 59 is close to the straight line of $\log\left(Nu/Nu_{FM}\right) = \log\left(St_c/St_{FM}\right)$ which passes through point (1.1) in the transition and continuum regime. The deviation of the curve from a straight line occurs at the beginning of the transition regime, and the reason is not quite clear at this time. But the generalized approach will be given later for this phenomena.

Figure 12 [43] shows the possibility of the existence of one dominating curve in the subsonic transition regime, which is the first indication of the interpolation formula.

4.3.1.   Accuracy of experimental data for sphere

The possible source of errors for measuring the total heat transfer coefficient is [43]:

1.   From the recording potentiometer (Max. 10 percent)

2.   From the time-history measurement (Max. 2.5 percent), for both the average overall convection coefficient $\left(h_c\right)$ and the average overall radiation coefficient $\left(h_r\right)$
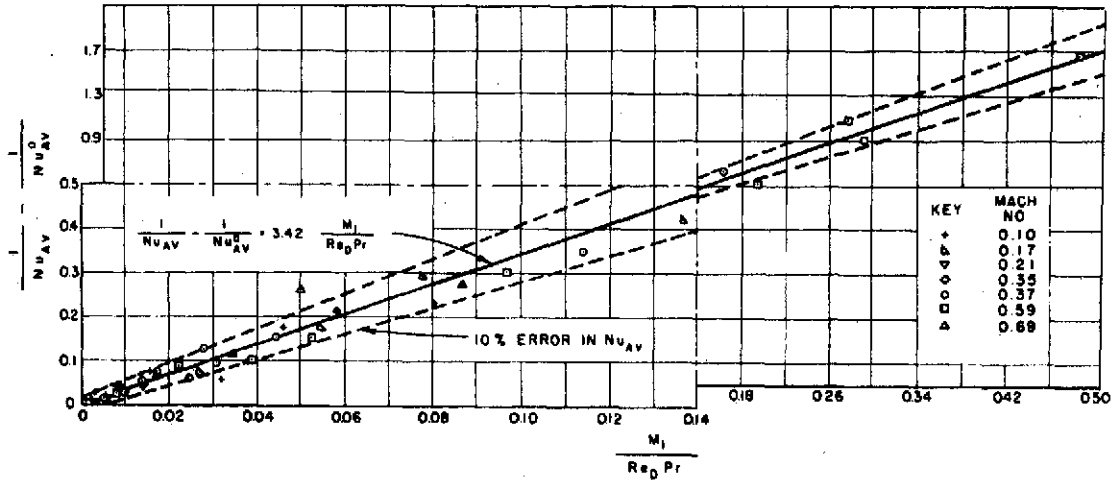
Fig. 12. Correlation of heat transfer from spheres in rarefied sub-
sonic air flow [43].

3. Due to radiation-conduction correction which amounts to 50

percent of the total heat transfer uncertainty $\left(h_c + h_r = \right.$

$\left. 25\% \right)$.

Therefore, the maximum uncertainty in the average convection heat

transfer coefficient $\left(h_c\right)$ is

$$25\% \times 0.5 + 12.5\% = 25\%$$

This uncertainty in h_c will be transmitted directly to the Nusselt

number, neglecting deviation of conductivity $(\partial k/k)$ and characteristic

length $(\partial L/L)$. The above discussion of uncertainty was reported in

reference 43. Analysis of the experimental data with respect to the

- 44 -

theoretical values, $Nu_T = 1/\left(1/Nu_c + 1/Nu_{FM}\right)$, shows that the maximum

uncertainty runs as high as 9.1 percent as shown in Fig. 13. This

phenomena suggests that the interpolation rule can be reasonably

applied to the data. Considering the scattering of the data in the

transition, and slip flow regimes, the actual uncertainty may be within

7 percent, which is close to the results of the cylinder.

4.4. Cylinder

Heat transfer from cylinders in the slip and transition regimes

produces effects similar to those described for spheres, as was pointed

out by many investigators, including Eckert and Drake [3].

Sauer and Drake [75] presented a theoretical formulation for

convection heat transfer from horizontal cylinders in a rarefied gas.

Their solution predicts the trend of the data satisfactorily. However,

some question remains regarding the representative magnitude.

Baldwin [76] presented some experimental data for the heat

transfer coefficient in the following range:

Mach number (M) 0.05 to 0.80

Reynolds number (Re) 1 to 75

Knudsen number (Kn) 0.009 to 0.077

Baldwin confirmed that his data and the theory of Sauer and Drake [75]

had the same trend but that the theory failed to fill the data quantita-

tively.

The data from Stalder [17] covers the range 2.0 < M < 3.3 and

0.28 < Re < 203. The Reynolds number is based on the free stream

conditions and cylinder diameter. Stalder [17] reported that heat

transfer data can be represented with an average deviation of ±6 per-

cent by the following relation:

- 45 -
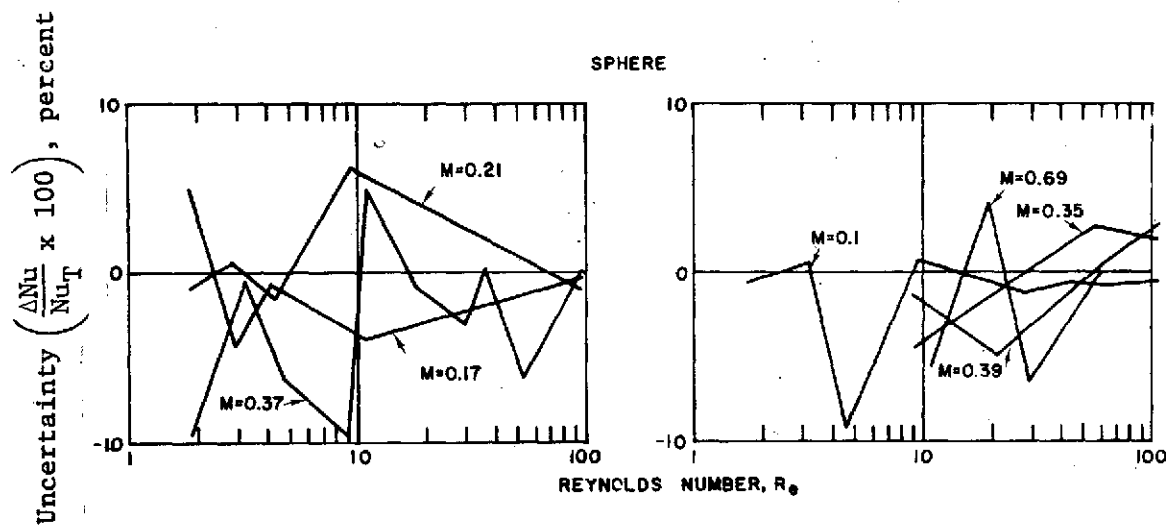
Fig. 13. Reynolds number versus heat transfer coefficient uncertainty, where $Nu_T = 1/(1/Nu_c + 1/Nu_f)$ ($\alpha = 0.85$).

$$Nu_{10} = 0.132 \, Re_{10}^{0.73} \tag{60}$$

where the subscript 10 refers to the fact that the viscosity and thermal conductivity were measured at tunnel stagnation temperature, and the density was elevated at free-stream conditions.

Equation 60 correctly represents the heat transfer data in the slip and transition regimes for cylinders in supersonic flow where the structure of the shock wave which forms in the rear of the cylinder is well established. This leads to the conclusion that Eq. 60 may not give satisfactory results if it is to be applied to the case of subsonic flow where no shock wave exists.

Kavanau [43] indicated that his analysis for heat transfer from spheres compared favorably to the results for cylinders. This indicates that Kavanau's analysis for heat transfer from spheres can be adequately applied to cylinders. Eckert and Drake [3] confirmed this fact by indicating that the heat transfer effects of spheres and cylinders are very similar.
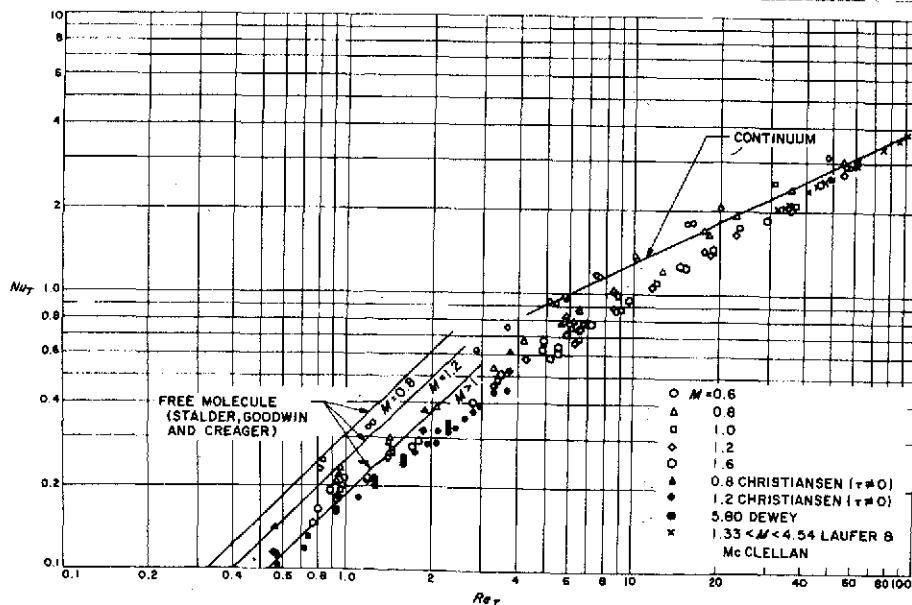
Fig. 14. Heat transfer from fine wires in transonic flow, T = 0 [33].
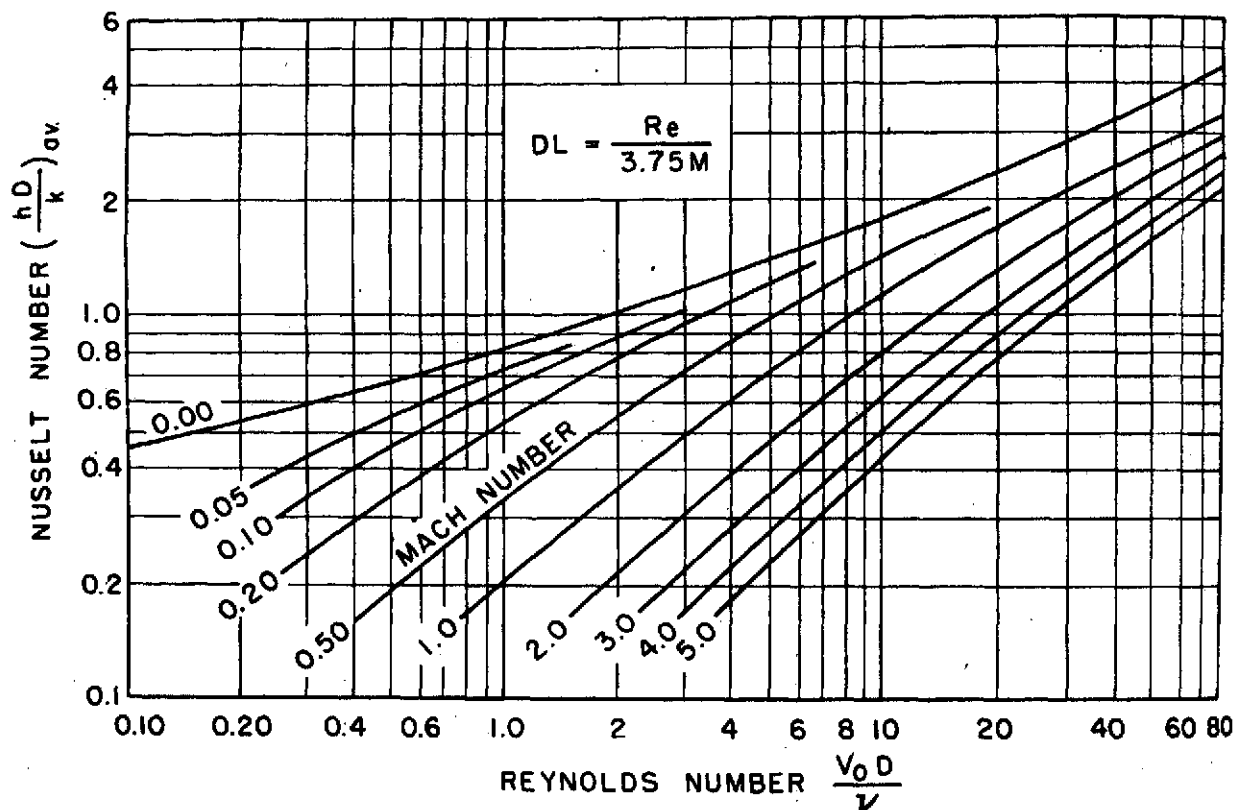
Fig. 15. Heat transfer coefficient for horizontal circular cylinders
in air showing variation with Mach and Reynolds numbers [75].

4.4.1. Accuracy of experimental data for cylinder (wire)

The accuracy of the heat transfer coefficient for cylinders is

the same as that of spheres in subsonic rarefied gas flow because of

the same characteristics of velocity and temperature distribution [3].

Uncertainty (or difference) between the theoretical value and experi-

mental data for rarefied gas region runs as high as 6 percent for sub-

sonic flows which occur in the slip flow regime. For selecting the

sample data, at least 2 percent errors exist in reading the plot Nu

versus Re.

As mentioned before, the interpolation rule

$$Nu_T = \cfrac{1}{\cfrac{1}{Nu_c} + \cfrac{1}{Nu_{FM}}} \qquad (58)$$

where

$$Nu_c = 0.43 + 0.48 \sqrt{Re} \qquad (14)$$

$$Nu_f = RePr \frac{\gamma + 1}{\gamma} \alpha \frac{1}{4\sqrt{\pi}} e^{-s^2/2} \left\{ \frac{1}{s} I_o \left(\frac{s^2}{2}\right) + s \left[I_o \left(\frac{s^2}{2}\right) + I_1 \left(\frac{s^2}{2}\right) \right] \right\}$$

$$s = \sqrt{\frac{\gamma}{2}} M \qquad (25)$$

was taken as a theoretical computation, where the input was the standard atmosphere [75].

Comparison of the results of Eqs. 14 and 25 and the experimental data is shown in Fig. 16. The uncertainty, $\Delta Nu/Nu_T \times 100$, is taken as a vertical axis, whereas Reynolds number is the horizontal axis, and Mach number is a parameter. The experimental data were taken from references 3, 7, 75, 34, and 78 for subsonic flow. The graph shows that the uncertainty increases as Mach number increases, reaching maximum ($\Delta Nu/Nu_T \times 100$) percent = 6.1 percent at $\mu = 0.8$ and Re $\simeq$ 13. As the experimental data were obtained from many authors, the plot scatters very widely, and the large spread in the data presents firm conclusions about the variation of the heat transfer coefficient with the Mach and Reynolds number. But this fact also serves to improve the maximum uncertainty to within 5 percent, rather than 6.1 percent for subsonic flows. Therefore, the interpolation formula, $Nu_T = 1/\left(1/Nu_c + 1/Nu_{FM}\right)$ is reasonably good to cover from free molecule flow through slip and transition up to the continuum regime.
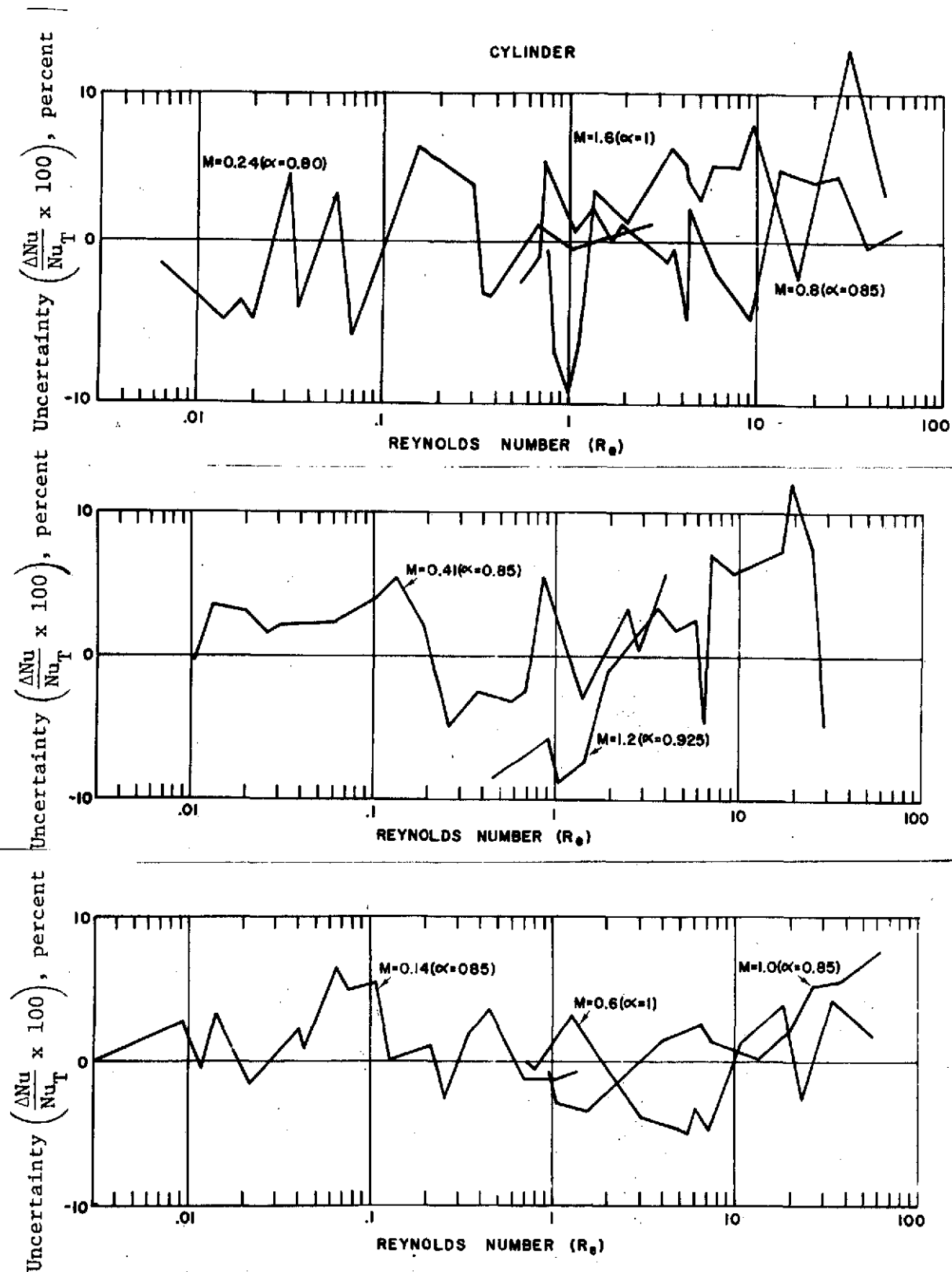
Fig. 16. Reynolds number versus heat transfer coefficient uncertainty,
where $Nu_T = 1/(1/Nu_e + 1/Nu_f)$.

5. General Trend of Uncertainty of the Heat Transfer Coefficients in Rarefied Subsonic Flow

The same argument discussed in Section 3 for the free molecule regime and transition regime can be drawn for flow perpendicular to a cylinder. For the slip flow regime, the same argument can be applied by the reasonably accurate calculation (the uncertainty in reading the experimental data is approximately 2 percent compared to the average heat transfer coefficient), i.e., the interpolation rule can be extended reasonably to the slip flow regime.

Experimental data and the free molecular theory depart from each other as they approach the slip flow regime. This departure is toward a reduction of momentum and energy exchange rates, which is expected as a consequence of slip and temperature jump effects at the surface. The reduction amounts to about 1 percent of Nu_{FM} when $Nu_c / Nu_{FM} \simeq 0.1$ [34].

In plots of Nu/Nu_{FM} versus Nu_c/Nu_{FM}, many transition experiments look alike, regardless of the body shape or quantity measured [34]. This suggests, for the plots of function ratio, that F/F_{FM} versus F_c/F_{FM}. By examining the plots, it was found that the body shape was not important in either continuum creeping flows ($R \ll 1$) or very low Mach number free molecule flow. Therefore, the dependence on body shape is negligible for subsonic transition flow. Summarizing the above argument, we deduce a very important interpolation formula, which applies adequately to the entire transition regime. The interpolation rule is

$$Nu = \frac{1}{\dfrac{1}{Nu_c} + \dfrac{1}{Nu_{FM}}} \qquad (58)$$

- 51 -

Equation 58 is purely deduced by observation of experimental data for all regimes (free molecule, transition, and continuum regime, respectively). By reasonably accurate calculation, the interpolation rule can also be extended to slip flow regime, as stated previously.

The following plots support the above argument very well.
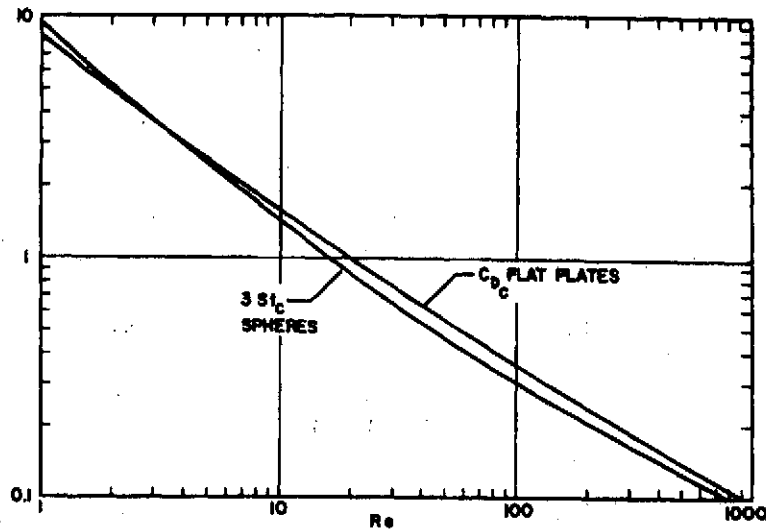
Fig. 17. Continuum coefficients [34].
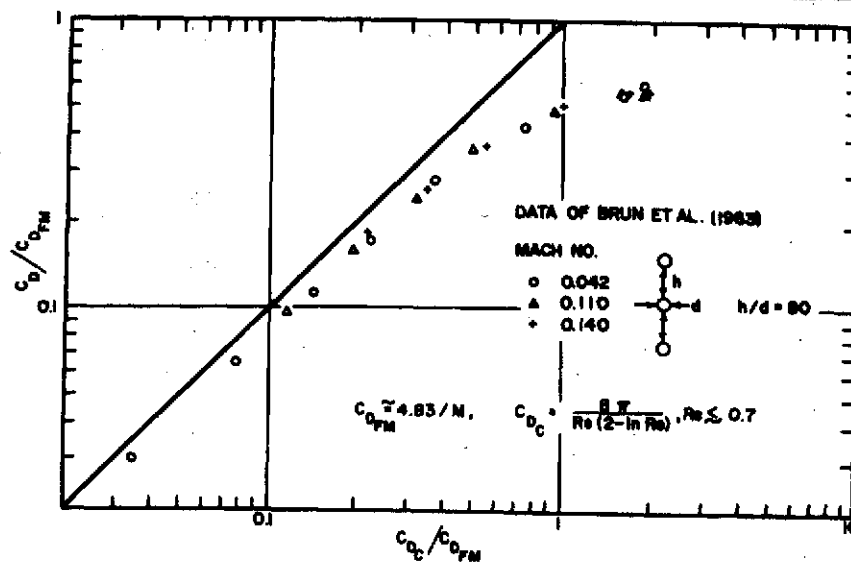
Fig. 18. Subsonic cylinder drag [34].

The above two curves are the experimental results for flat plate drag coefficients and Stanton number variation for spheres in the subsonic transition regime. Surprisingly, Eq. 57 applies well to these curves. By this analogy, if we define the following parameters,

$F = F(Re,M)$ = any dimensionless characteristic quantity which is a function of both Re and M.

$F_{FM} = F_{FM}(M)$ = function only of Mach number. Geometry is not important for the free molecule flow.

$F = F_c(Re)$ = function only of Re in subsonic continuum regime as M $\rightarrow \infty$. (61)

then, any characteristic quantity for the subsonic transition regime can be formulated by

$$F(Re,M) = \frac{1}{\dfrac{1}{F_{FM}(M)} + \dfrac{1}{F_c(Re)}}$$ (62)

$F(Re,M)$ for transition regime would be any characteristic quantity, say, Stanton number $\left[St(Re,M)\right]$, drag coefficient $\left[C_D(Re,M)\right]$, or Nusselt number $\left[Nu(Re,M)\right]$, etc. Equation 58, the heat transfer interpolation rule for the transition regime, accurately represents the departure between continuum and slip flow regime, and also that of the free molecule and transition regime [34]. The inaccuracy of this interpolation formula for all regimes in subsonic flows runs as high as 7 percent for spheres and 5 percent for cylinders, as shown in Figs. 13 and 16, respectively.

RECOVERY FACTOR

1. Introduction

The direct measurement of static temperature T_∞ in a moving fluid is of great importance in heat transfer measurements. The temperature indicated by any thermometer immersed in the fluid is higher than the static temperature, for there is an increase of temperature through the boundary layer from the static temperature at the edge of the boundary layer to the recovery temperature T_r at the surface.

T_r will, in general, be different on different parts of the surface, depending on geometry, Reynolds number, etc., and the thermometer will indicate a mean recovery temperature.

The recovery temperature is expressed nondimensionally by a recovery factor r defined by the equation [3]

$$T_r - T_\infty = r \frac{u^2}{2Cp} \tag{63}$$

or, in other terms, the recovery factor is usually defined as

$$r = \frac{T_r - T_\infty}{T_o - T_\infty} \tag{64}$$

where the subscript o refers to the stagnation condition. The accurate determination of the recovery factor is very important in heat transfer measurements, recovery temperature and heat flux.

The following discussion concerns determination of the recovery

factor in the continuum, slip and transition, and free molecular
regimes for the flat plate, cylinder, and sphere.

2. Continuum Flow

2.1. Flat Plate

2.1.1. Laminar boundary layer on a flat plate

The energy equation which describes heat transfer in a laminar,
steady boundary layer, including the effect of internal friction is [3]

$$u \frac{\partial T}{\partial x} + v \frac{\partial T}{\partial y} = \alpha \frac{\partial^2 T}{\partial y^2} + \frac{\mu}{\rho C_p} \left(\frac{\partial y}{\partial y}\right)^2 \qquad (65)$$

The situation to be considered first is the one with an adiabatic
surface. The boundary condition is

$$\frac{dT}{dy} = 0, \quad \text{at } y = 0$$

$$T = T_\infty \quad \text{at } y = \infty$$

The recovery field is identical with that of low flow velocities as
long as the properties are considered constant. A solution to the
problem to determine the temperature field in the boundary layer was
obtained for the first time by Pohlhausen [6]. A transformation to a
total differential equation is possible by introduction of the parameters
f and η and by use of the following parameter,

$$\zeta_r = \frac{T - T_\infty}{u_\infty^2/2C}$$

which expresses the temperature field in the boundary layer in a dimensionless form. Noting that

$$\eta = \frac{1}{2} y \sqrt{\frac{u_\infty}{\nu x}}$$

and

$$f(\eta) = \frac{\Psi}{\sqrt{\nu u_\infty x}}$$

where

Ψ = stream function

Equation 65 becomes

$$\frac{d^2 \zeta_r}{d\eta^2} + Pr\ f\ \frac{d\zeta_r}{d\eta} + \frac{Pr}{2} \frac{d^2 f}{d\eta^2} = 0 \tag{66}$$

A solution of this equation can be obtained by the method of variation of coefficients and results in

$$\zeta_r = \frac{Pr}{2} \int_o^\infty \Phi d\eta - \frac{Pr}{2} \int_o^\eta \Phi d\eta \tag{66.a}$$

where

$$\Phi = \exp\left(- Pr \int_o^\eta f d\eta\right) \left[\int_o^\eta \left(\frac{d^2 f}{d\eta^2}\right)^2 \exp\left(Pr \int_o^\eta f d\eta\right) d\eta\right] \tag{67}$$

The assumed plate surface temperature is its recovery temperature, and the value of the parameter ζ_r at the wall is equal to the recovery

factor r. The recovery factor is, therefore,

$$r = \frac{Pr}{2} \int_0^\infty \exp\left(- Pr \int_0^\eta f d\eta\right) \left[\int_0^\eta \left(\frac{d^2 f}{d\eta^2}\right)^2 \exp\left(Pr \int_0^\eta f d\eta\right) d\eta\right] d\eta \qquad (68)$$

Values of the recovery factor have been obtained by numerical integration of this equation. Busemann [3] has shown that these values can be approximated in the Prandtl number range from 0.5 to 5 by the simple expression

$$r = \sqrt{Pr} \qquad (69)$$

For low velocity boundary layer, the heat flow at the plate surface per unit area and time is determined by the difference between the actual wall temperature and the temperature of the free stream outside the boundary layer. The heat flow in a high-velocity boundary layer is given by the same relation as the heat flow in a low-velocity boundary layer except that the temperature potential determining the heat flux for high velocity is the difference between the actual wall temperature and its recovery temperature.

For high velocity boundary layer [3]

$$q = k\left(\frac{\partial \theta'}{\partial y}\right)_\omega \left(T_\omega - T_r\right)$$

For low velocity boundary layer,

$$q = k\left(\frac{\partial \theta'}{\partial y}\right)_\omega \left(T_\omega - T_\infty\right)$$

where

$$\theta' = \frac{\displaystyle\int_0^\eta e^{-\left(\int_0^\eta \mathrm{Pr}\, f d\eta\right)} d\eta}{\displaystyle\int_0^\infty e^{-\left(\int_0^\eta \mathrm{Pr}\, f d\eta\right)} d\eta} \tag{70}$$

2.1.2. Turbulent boundary layer over a flat plate

Since the energy equation for the boundary layer is linear in temperature, then all the relations derived for the determination of heat flow over a flat plate for the laminar boundary layer with low velocity apply for high velocity after replacing the free stream temperature by the recovery temperature. This rule holds also for the turbulent boundary layer. The only additional knowledge required is that of the recovery factor for the particular situation, from which the recovery temperature can be determined. For turbulent flow, the following relation has been derived theoretically [79] and verified for Prandtl values near 1 [3].

$$r = (\mathrm{Pr})^{1/3} \tag{71}$$

It has been established that the heat transfer relation for a constant property fluid approximates the conditions in high velocity flow of gases provided the pressure in the flow field is constant and the property values are introduced at an appropriately chosen reference temperature.

It was found that the relation $r = \sqrt{\mathrm{Pr}}$ accurately describes the

results of the calculations for gases with variable properties, provided

the temperature differences $T_r - T_\infty$ (when T_∞ = static temperature) are

such that the variation of specific heats in this temperature range can

be neglected [5]. For very large supersonic velocities, when the varia-

tion of the specific heats becomes important, the Prandtl number is

introduced at a reference enthalpy [3]

$$i^* = i_\infty + 0.72\left(i_r - i_\infty\right) \qquad (72)$$

In laminar flow at a moderate temperature, the recovery factor

is 0.84. For the turbulent boundary layer flow of air over a flat

plate, a value of 0.88 was measured [3]. In the transition region

between laminar and turbulent boundary layers, the recovery factor

rises from the value of 0.845 to a peak 0.89 and then decreases to

the turbulent value of 0.88 as seen in Fig. 19.
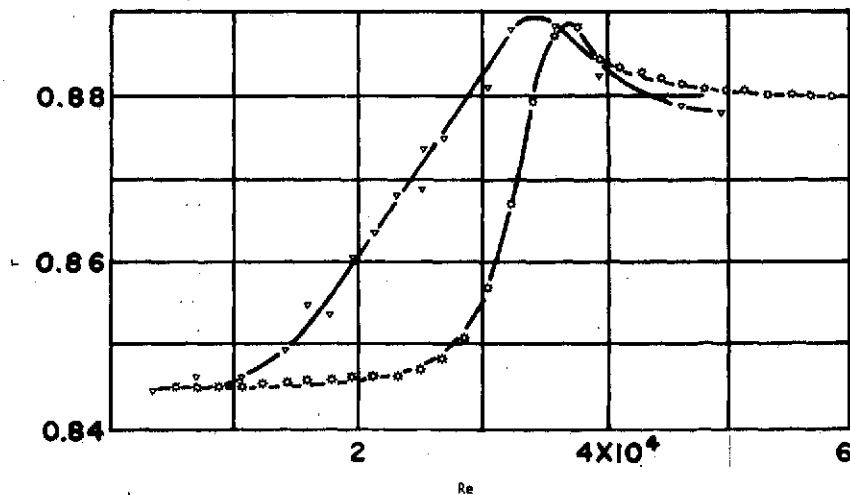
Fig. 19. Laminar transitional and turbulent temperature-recovery
factors r for a (measured on a cone at M = 3.12): [80]

a. High stream turbulence
b. Low stream turbulence

Van Driest [5] made the assumption $\mu\rho$ = constant as a first approximation, and employed a method of successive approximations. The solution is developed for a gas with Pr = 0.75, constant properties, γ = 1.40, and the Sutherland law for viscosity. Despite the temperature dependence of the fluid properties, the equation $r = \sqrt{Pr}$ is again found to be a good approximation [3].

As discussed above, in laminar flow $r = (Pr)^{1/2} = 0.845$ for air; and in turbulent air flow, $r = (Pr)^{1/3} = 0.88$. Experimental values confirm the above equations very well, and uncertainties are approximately 1 percent for both cases; i.e., uncertainty for laminar flow $= \frac{0.005}{0.845}$ x 100 percent $\approx$ 1 percent, and for turbulent flow $= \frac{0.005}{0.880}$ x 100 percent $\approx$ 1 percent.

2.2. Cylindrical Body

Some confusion exists concerning the recovery factor values for blunt bodies (cylindrical, circular, etc.).

Thompson [81] was interested in the low velocity case. His experimental data for thermistors yields recovery factor values between 0.70 and 0.80. The results of Thomson were closely matched by the results obtained by Hottel and Kalitinsky [82], which are also reported by Moffat [83]. Hottel and Kalitinsky [82] obtained the following values for low speed flow:

For wires normal to flow; $r = 0.68 \pm 0.07$

For wires parallel to flow; $r = 0.86 \pm 0.09$

They also reported recovery factor values for small thermocouple balls attached to very thin wires. Values of 0.74 with normal flow and 0.78 with parallel flow [76] were reported.

2.2.1. Degree of accuracy for cylindrical body

The results mentioned above reveal an inconsistency in the recovery factor values for wires normal to the flow in subsonic flow and supersonic flow. Many investigators agree [43, 82, 83] that the proper value for the recovery factor in supersonic flow is about 0.85 and that Mach number has no effect on recovery factor. The disagreement, however, involves the correct value for r in the subsonic flow. If one chooses the value of 0.85 for r in the supersonic regime and the value of 0.68 in the subsonic regime, an abrupt discontinuity exists at Mach number unity. Since many investigators agree that r is independent of Mach number variation and that there is no slow change detected in the neighborhood of Mach number unity, then this is not physically possible.

On the other hand, Schubuer and Tchen [84] reviewed the experimental results of many investigators in both subsonic and supersonic flow regimes, and reported that the recovery factor for cylindrical bodies in laminar flow has the value of 0.85 for both subsonic and supersonic regimes. Haworth [85] indicated that the recovery factor for blunt bodies has the value of 0.85 in laminar flow. Van Driest [5] pointed to this same conclusion.

Hottel and Kalitinsky [82] pointed out that their data for subsonic flow showed no effect of Mach number variation on the recovery factor values. This important conclusion was also pointed out by Schubuer and Tchen [84], who indicated that in their reviews of experimental data of many investigators in both subsonic and supersonic regimes, they found practically little or no change in the recovery

factor values due to Mach number. It was pointed out by Kavanau [43] and Atassi and Brun [21] that at low speeeds, the difference between the adiabatic wire temperature T_r and the gas stagnation temperature T_e, is no more than a few degrees centigrade. Therefore, it is difficult to determine the recovery factor with sufficient accuracy by direct measurement of the adiabatic wire temperature.

It is believed that the recovery factor value for wire in normal flow should be taken as 0.85 in laminar flow and 0.88 in turbulent flow in both the subsonic and supersonic regions, respectively. Therefore, it is believed that the values obtained by Hottel and Kalitinsky [82] and Thomson [81] are in error.

Some investigators [3] indicated that the results of measurements on a cylinder in a subsonic air flow normal to its axis yield recovery factors at the leading edge up to values approaching unity at the stagnation point. Actually, the recovery factor does not vary significantly from 0.84 or 0.88, recommended for laminar or turbulent flow, respectively. The reason for the erroneous conclusion reached in reference 5 is that the recovery temperatures for leading edge surfaces are higher than for other areas of the body for a given speed and ambient altitude conditions. This has been misinterpreted as being the result of an increase in the recovery factor at the leading edge.

The reason for the higher recovery temperature at the leading edge surface is due to the fact that the local static temperature is considerably higher because of the adiabatically compressed flow region in this area [87].

Uncertainty calculations for both laminar and turbulent flow are as follows for a cylinder parallel to the flow:

Laminar (both subsonic and supersonic) uncertainty $= \dfrac{0.05}{0.85} \times$ 100 $\simeq$ 6 percent.

Turbulent (both subsonic and supersonic) uncertainty $= \dfrac{0.05}{0.88} \times$ 100 $\simeq$ 5 percent.

These values are purely empirical, and corrected by several investigators. Also, the uncertainty may come mainly from the reading error of the data and instruments. If we consider this effect, the actual error would be smaller than that reported.

2.3. Spherical Body

It was pointed out by Haworth [86] and Eckert and Drake [3] that the shapes of the flow around spherical and cylindrical bodies are similar. This leads to the conclusion that the above discussion concerning cylindrical bodies applies as well to spheres. Haworth [86] suggested the value of 0.85 for the recovery factor in laminar flow, regardless of Mach number. Eckert and Drake [3] and Van Driest [5] suggested the same value of 0.85. Beckwith and Gallagher [87] showed that at any point around the spherical body, the recovery factor values closely follow the value given by the laminar boundary layer $r = \sqrt{Pr}$ when the flow is laminar, or the value given by the turbulent boundary layer $r = (Pr)^{1/3}$ for turbulent flow.

2.3.1. Degree of accuracy for sphere

For continuum flow, the recovery factor is given by the relation $r = (Pr)^{1/2}$ for laminar flow, and by $r = (Pr)^{1/3}$ for turbulent flow.

Measurements for the laminar recovery factor show a close agreement with the relation $r = (Pr)^{1/2} = 0.845$ as shown by Van Driest [5] and Haworth [86]. Experimental data for laminar flow by Schubuer and Tchen [84] and Haworth [86] show that the laminar recovery factor values are between 0.825 and 0.865. The data also indicates that the turbulent recovery factor varies between 0.875 and 0.890 in close agreement with the relation $r = (Pr)^{1/3} = 0.88$. Figure 20 shows the argument mentioned above for various cones. Many investigators agree that the general trend of the recovery factor of spheres is similar to that of flat plates.

The uncertainty calculations are:

Laminar flow: $r = 0.85 \pm 0.04$

$$\text{uncertainty} = \frac{0.865 - 0.825}{0.85} \times 100 \approx 4 \text{ percent}$$

Turbulent flow: $r = 0.88 \pm 0.02$

$$\text{uncertainty} = \frac{0.890 - 0.875}{0.88} \times 100 \approx 3 \text{ percent}$$

The uncertainty ranges were taken from the experimental data.

3. Free Molecule Flow

Heat transfer from a body to a rarefied gas stream in the Maxwellian equilibrium velocity distribution can be calculated entirely from the fundamental notions of the kinetic theory of gases. The results can be shown as a function of the ratio of the specific heats, and are generally in good agreement with the experimental data, so far as the molecular structure of the gas is concerned [1, 58, 59]. It was shown by Oppenheim [16] that the determination of correlated results for a few fundamental shapes such as flat plates, horizontal circular
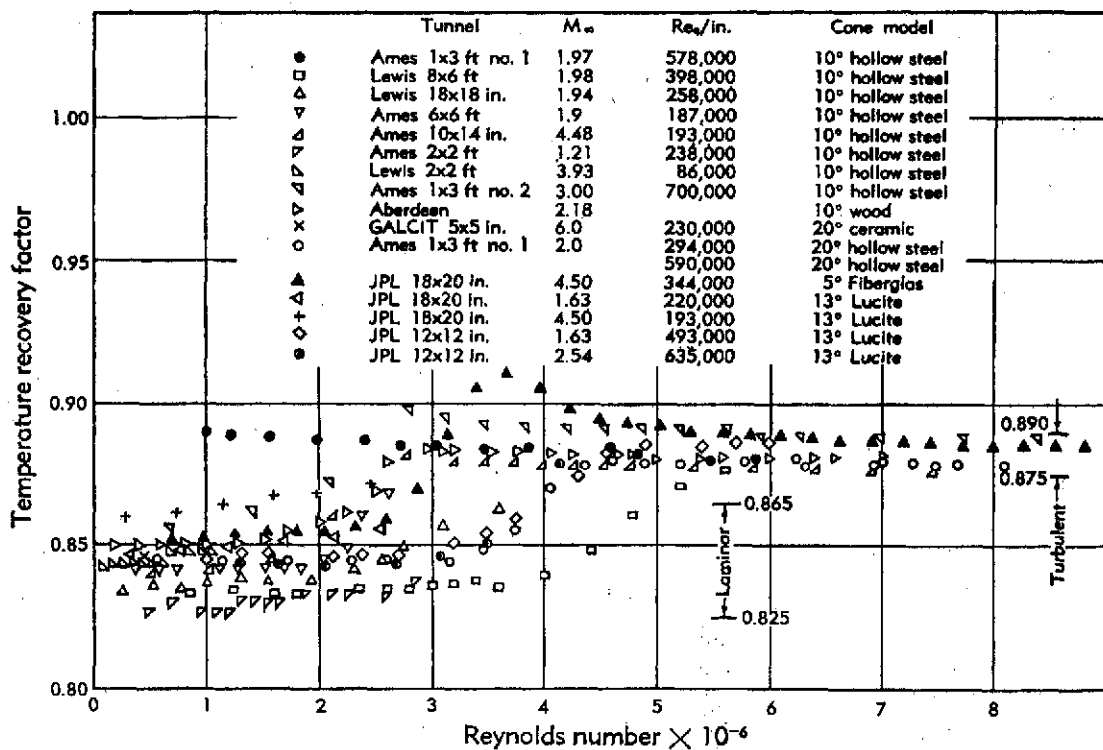
Fig. 20. Variation of the temperature recovery factor of cones with the Reynolds number. The Reynolds number is based upon the distance from the cone tip and on the conditions at the edge of the boundary layer. [84]

cylinders, and spheres will enable the formation of results for more complicated cases, by synthesis of the results of these simple shapes. The heat transfer in the free molecule flow is represented in terms of the Stanton number and the thermal-recovery factor. An expression for the thermal-recovery temperature T_r in the instance where T_{wall} = const., is obtained when the heat transfer θ is taken to be zero in the derived equations.

In such a case, the recovery factor is [16],

$$r = \frac{T_r - T_\infty}{T_o - T_\infty} = \frac{\gamma}{\gamma + 1} \left(2 + \frac{1}{s^2} \frac{\overline{F}}{\overline{G} + \overline{F}} \right) \tag{73}$$

where

$$\overline{G} = \frac{1}{A} \int_A \left(\frac{e^{-\eta^2}}{2s\sqrt{\pi}} \right) dA$$

and

$$\overline{F} = \frac{1}{A} \int_A \frac{\eta(1 + \mathrm{erf}\eta)}{2s} \, dA$$

A = area of the shapes

$\eta = \overline{U}_\eta / \overline{V}$

$\overline{U}_\eta$ = component of mass flow velocity normal to the wall

$\overline{V}$ = mean molecular velocity

$S = u/\overline{V} = \sqrt{\frac{\gamma}{2}} M$; molecular speed ratio related to Mach number M

Figures 21 and 22 show the thermal-recovery factors for a flat plate, a sphere, and a transverse circular cylinder in a free molecule

- 66 -
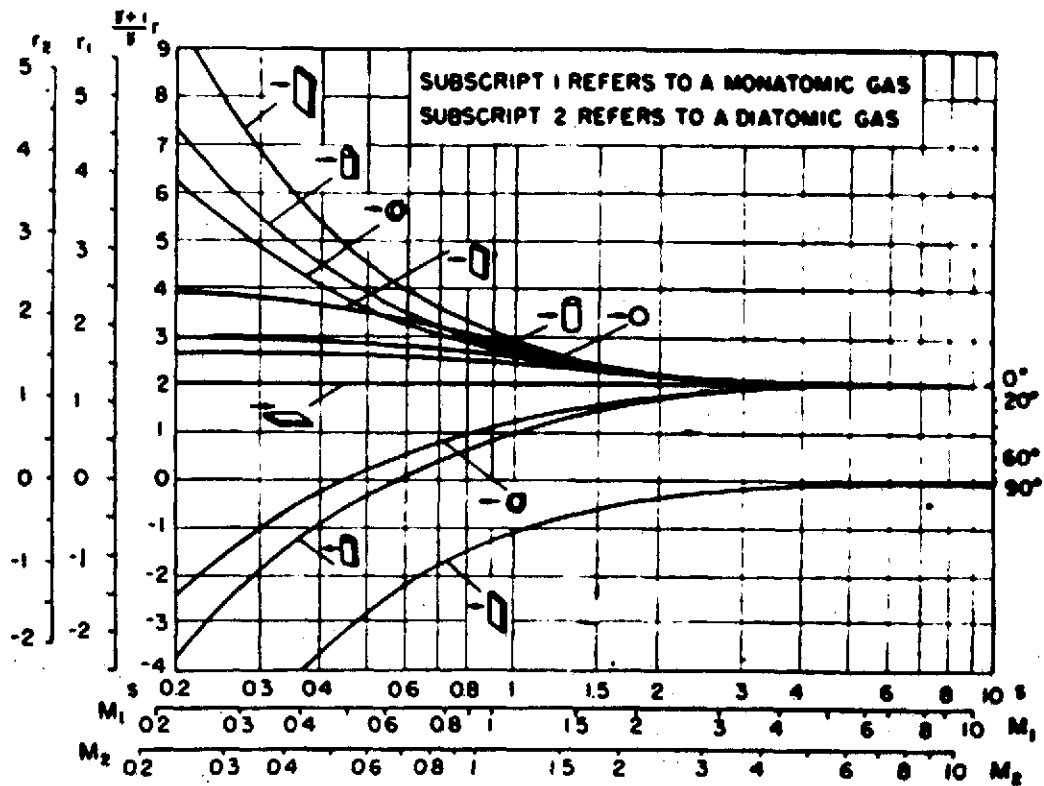
Fig. 21. Thermal-recovery factors for a flat plate, a sphere, and a transverse circular cylinder in a free molecule flow. [16]
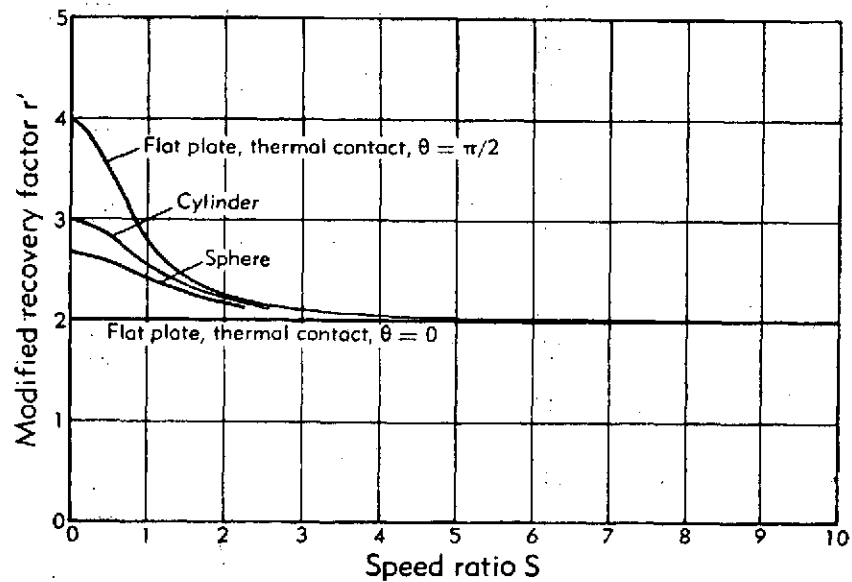
Fig. 22. Modified recovery factor in free molecule flow. [1]

flow as a function of the speed ratio. They also clearly show that the recovery factor in free molecule flow for a flat plate at zero angle of attack is constant for all values of speed ratio and Mach number, while the recovery factor values for sphere, cylinder and the flat plate at an angle of attack is a function of the speed ratio. However, the recovery factor values of a sphere, cylinder and flat plate at an angle of attack approach the value of the flat plate at zero angle of attack at high Mach numbers. For low Mach number in the free molecule flow, recovery factor for the sphere and cylinder is constant.

It should be noted that the flat-plate results apply to any surface making a constant angle with the flow. Therefore, these results apply to wedges and cones in comparison with the flat plates at angles of incidence with the flow, where the angle of incidence of the plate corresponds to half the opening angle of the wedge or cone. The zero-angle-flat plate corresponds to conditions occurring on a cylinder of any cross-sectional shape in axial flow.

A flat plate inclined at an angle of incidence θ to the direction of flow can be treated in terms of the flat plate normal to the flow, then

$$r_\theta(s) = \frac{2\gamma}{\gamma + 1} \cos^2\theta + r_n(\eta) \sin^2\theta \qquad (74)$$

where

$$\eta = s \sin\theta$$

subscript n = a flat plate normal to the flow

$$\gamma = \frac{C_p}{C_V}$$

- 68 -

Generally, r_{plate} (parallel flow) $< r_{cyl}$ (parallel flow) $< r_{cyl}$ (cross flow). Equation 73 indicates that for the case of flat plate at an angle of attack, the recovery factor in the free molecular regime is a function of both the speed rate and the angle of attack [3, 16, 73].

3.1. Degree of Accuracy

Experimental data of Stalder [17] for transverse cylinders in supersonic flow and the data of Drake and Backer [74] seems to confirm the Oppenheim theory [16]. For a sphere in supersonic flow, Drake and Backer [74] found that the overall recovery factors, when plotted against $\sqrt{Re}/M$, were shown to increase to values above unity at values of $\sqrt{Re}/M < 5$; whereas at $\sqrt{Re}/M > 5$, the recovery factors were shown to remain practically constant at a value $r = 0.90 \pm 0.03$. Therefore, the uncertainty for $\sqrt{Re}/M > 5$ runs as high as 3 percent [74]. This effect is one associated with the transition region, and is not the result of nonadiabatic gas flow.

4. Transition and Slip Flow Regimes

4.1. Introduction

Contrary to the situation in the continuum and free molecule flow regimes, there are no dependable theories to analyze and predict the heat transfer and recovery temperature in the slip and transition flow regimes. Experimental data in these two regimes is not very helpful either.

There are some experimental data for the recovery factor in supersonic flow for some geometrical shapes [17, 74, 33], but there are very little data for subsonic flow [21, 33].

Experimental data for cylinders and spheres show that the rarefaction effects begin to show at about Kn ≃ 0.02. Drake and Backer [74] reported that the recovery factors start to depart from the continuum flow values at about $Re_2/M_2 \simeq 20$, where the subscript 2 refers to conditions after the detached shock [88].

Figure 23 indicates that the recovery factors at values of $\sqrt{Re_1}/M_1$ > 5 are essentially constant at a value of 0.93 ± 3 percent, where the
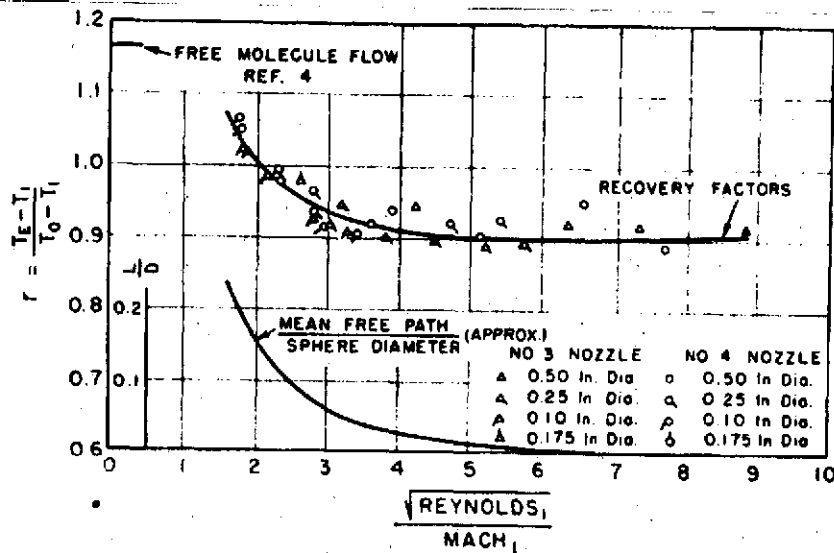
Fig. 23. Variation of thermal recovery factor for spheres in a transition flow regime [74].

subscript 1 refers to conditions before the detached shock and where $Re_2/M_2 \simeq 4Re_2/M_1$. At $\sqrt{Re_1}/M_1$ < 5, however, and as $\sqrt{Re_1}/M_1 \to 0$, the values of the recovery factor increase rather sharply to values greater than unity, indicating that the recovery temperature attained by a sphere in a stream of gas at a large Mach number is greater than the total temperature of the flow.

The data of Stalder [17], which is shown in Fig. 24, shows that fully developed free molecule flow occurs for Kn of approximately 2.0
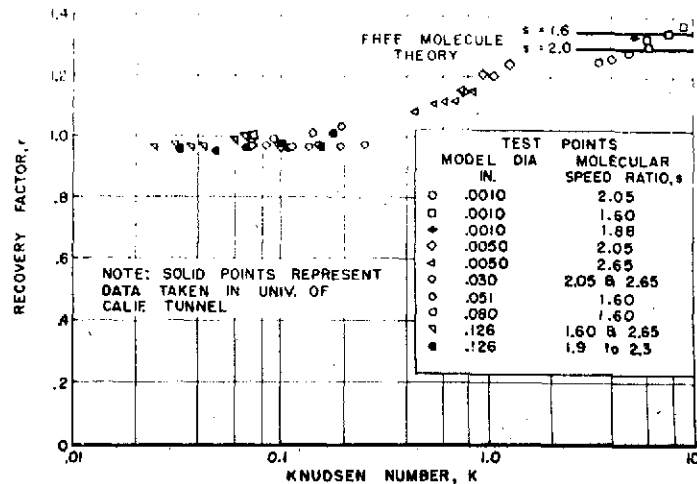
Fig. 24.   Thermal recovery factor for transverse cylinders in supersonic
flow [17].

and higher, and that for Kn ≥ 0.2, the recovery factor r exceeds unity

even though the free-molecular flow is not fully developed.   Figure 24

also shows that the data in the range of Kn from 0.2 to 2.0 are

corrected by Kn alone with no systemetric Mach number effects shown.

Further, it is evident that for values of Kn > 0.2, the recovery factor

exceeds the value of unity, presumably due to the development of free-

molecular flow effects.   The experimental data clearly show the trend

of the recovery factor in the slip and transition regimes.   The recovery

factor is equal to that of the continuum flow and stays constant for

slight increases in rarefaction effects.   Then these rarefaction effects

start to increase the recovery factor asymptotically until it approaches

the value which corresponds to the free-molecular regime.

Vrebalovich [33] reported a collection of experimental recovery

factor data for both supersonic and subsonic flow.   These data are shown

in Fig. 25, where

$$\eta^* = \frac{\eta - \eta_c}{\eta_{FM} - \eta_c}$$

$$\eta = \frac{T_r}{T_o} = \frac{\text{Recovery temperature}}{\text{Stagnation temperature}} \tag{75}$$
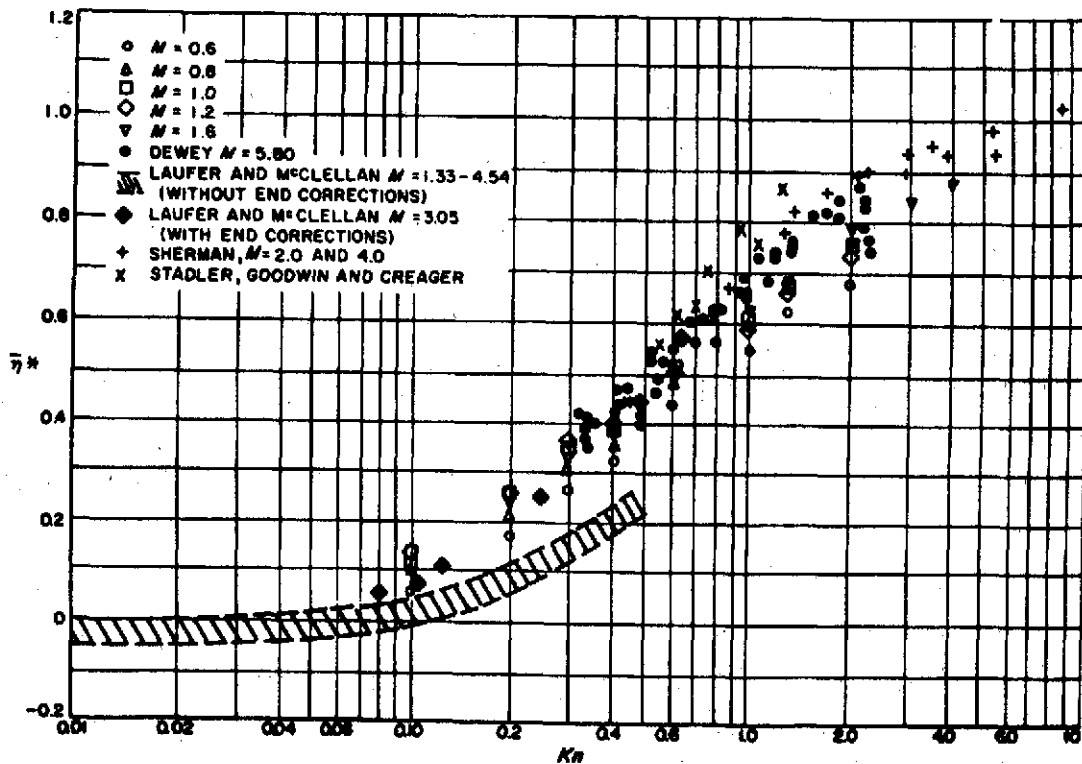
Fig. 25. Normalized recovery ratio versus free stream Knudsen number [33].

Figure 25 shows the same trend as Fig. 24. The supersonic flow
data show that in the slip and transition regimes, the recovery factor
is mainly dependent on Knudsen number and that Mach number has no effect.
However, the recovery factor data clearly indicate that Mach number has

- 72 -

a profound effect in the subsonic flow. The data show that for any

Knudsen number in the slip or transition regimes, Mach number increases

cause a corresponding increase in the recovery factor value.

Attasi and Brun [21] reported some recovery factor data for

wires at low Mach numbers. This data indicate the same trend shown by

Stalder [17] and Vrebalovich [33]. However, their data yield higher

values for the recovery factor in the slip and transition regime than

those reported by Vrebalovich [33] for the same Mach numbers. This

discrepancy is not surprising at low Mach numbers because it is very

difficult to determine the recovery factor with sufficient accuracy

at low Mach number [33, 43]. The data of Vrebalovich [33] is more

consistent, which gives more confidence in its accuracy. His experi-

ment is successful with only 1 percent error at $Re_T = 0.5$, $M = 0.6$

for a cylinder [33]. The curves presented are faired from the experi-

mental data by the variable, $\eta = T_r/T_o$, where

T_r = recovery temperature of infinite length

T_o = stagnation temperature

and are very close to the results of Kovasnay [89], in which he con-

sidered end loss corrections of the cylinder at low Reynolds numbers.

This aspect is shown in Fig. 26.
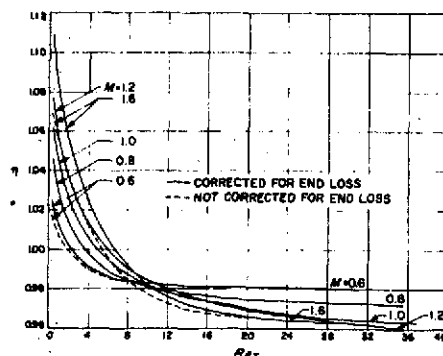
Fig. 26. Recovery temperature ratio in transonic flow [33].

4.2. Sphere

Figure 27 shows the thermal recovery factor r versus Reynolds number for spheres in supersonic flow. The uncertainty runs as high as 5 percent.
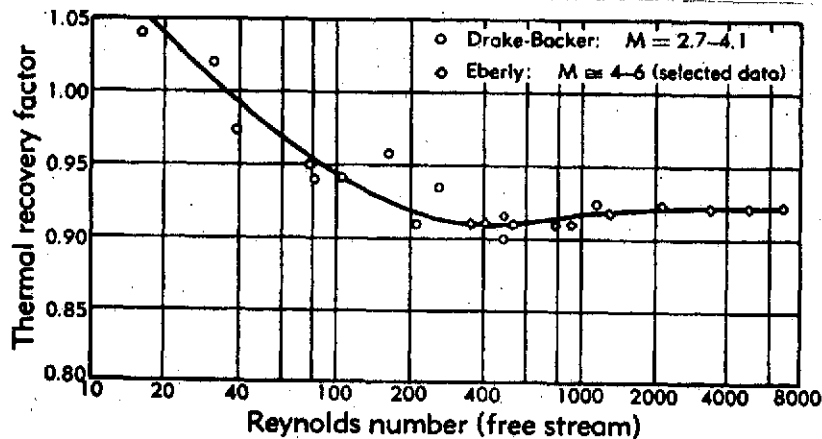
Fig. 27. Thermal recovery factor for spheres in supersonic flow [1].

4.3. Cylinder

Figures 26 and 27 show r versus Kn for different model diameters. The effect of the increase of rarefaction on the trend of r as it approaches the free-molecular value is apparent. The uncertainty of the data runs as high as 4 percent. These data were taken for cylinders held normal to the stream.

4.4. Flat Plate

Laminar slip flow over a flat plate at zero angle of attack can be treated in terms of the Rayleigh problem of an impulsively started plate. The inertia and viscous terms in the Navier-Stokes equations can be simplified in this case. Since a reliable method for extending boundary layer theory to lower Reynolds numbers is not yet available, and very little reliable heat transfer experimental data for the case of the flat plate are available at the present time, an approximate solution is ne-

cessitated.

In a private communication, Morrissey [91] reported an empirical
formula used to interpolate from the free molecular recovery factors
to the continuum recovery factors as a function of the Knudsen number.

$$r = r_c + \frac{Kn\left(r_{FM} - r_c\right)}{Kn + 0.3} \tag{76}$$

where

r_c = continuum flow recovery factor

= 0.88 for turbulent flow

= 0.845 for laminar flow

and

r_{FM} = free molecular flow recovery factor

The free molecular recovery factor depends on the geometrical shape
and the speed ratio which was mentioned in Oppenheim's theory.

Koshmarov [92] obtained a similar relation from his own heat
transfer experimental data involving a sharp cone. By plotting

$$\frac{r - r_c}{r_{FM} - r} \quad \text{versus} \quad \frac{M \, \mu_e \, T}{Re \, \mu \, T_e}$$

he obtained a series of parallel straight lines with the half angle at
the cone apex as a parameter. The subscript e refers to the total
equilibrium condition, while the quantities with no subscript refer to
the undisturbed flow far away from the cone.

The recovery factor in the transition regime is, as shown in
Eq. 76, a function of the Knudsen number. It is also a function of the
speed ratio and the angle of attack in the same manner discussed before

regarding the free-molecular recovery factor. Equation 76 was apparently obtained by smoothing out the existing experimental data in the slip and transition regimes. This equation compares well with the existing recovery factor data in supersonic flow [17, 33]. However, the comparison does not seem to be very good in the case of subsonic recovery factor data. In this case, Eq. 76 yields values higher than the reported experimental values. A better adjustment might be obtained if the constant 0.30 in the denominator of Eq. 76 were changed to a slightly higher value.

Some investigators [81, 82] reported their data in terms of $\left[\dfrac{r - r_c}{r_{FM} - r_c}\right]$ versus Kn. It should be expected that the quantity $\left(\dfrac{r - r_c}{r_{FM} - r_c}\right)$ is a function of Knudsen number, Mach number and angle of attack. The dependence on Mach number and angle of attack is apparent since the free molecule recovery factor r_{FM} is a function of both the Mach number and the angle of attack. The dependence of r_{FM} on the Mach number is pronounced in the subsonic flow. This leads to the conclusion that Eq. 76 should be written as

$$\frac{r - r_c}{r_{FM} - r_c} = \frac{Kn}{Kn + c} \tag{77}$$

where the parameter c is a function of Mach number. Morrissey [91] chooses the numerical value 0.3 for c, which makes Eq. 77 agree with the supersonic data. For low Mach numbers the value of c seems to vary from 0.5 to 0.9, for Mach numbers 0.9 to 0.1, respectively. Oman and Scheuing [57] obtained the following closed form expression for the recovery factor in laminar slip flow over a flat plate for Pr = 0.72 and thermal accommodation coefficient $\alpha = 0.9$

$$r = [4\gamma/(\gamma + 1)] \; [\alpha/(2-\alpha)] \left[\frac{u_s}{u_\infty}\right]^2 + \sqrt{Pr} \left[1 - \left(u_s/u_\infty\right)^2\right]$$

As u_s/u_∞ increases toward the free molecule value, r increases to a value greater than unity. The assumptions involved, therefore, appear to account for the predominant slip flow effects.

4.5. Degree of Accuracy

The uncertainty in the value of the recovery factor in the slip and transition flow regime may be argued as follows:

a. The reported data for the recovery factor in the transition regime seem to have a maximum uncertainty of 5 percent, which is the ratio of the difference between the experimental and theoretical values to the theoretical value [17].

b. If it is decided to use Eq. 77 to obtain the recovery factor in the transition regime, then, since r in the transition regime depends on r_{FM} and r_c, its uncertainty depends on the uncertainty of both r_{FM} and r_c. In Eq. 77, if the turbulent value of 0.880 is used for the continuum recovery factor, then the reported data fall between 0.825 and 0.865. With respect to the free-molecular recovery factor, experimental data agree with the Oppenheim theory. Combining the uncertainty in both the continuum and free molecular recovery factors yields the conclusion that the uncertainty in the recovery factors in the transition regime might run as high as 7 percent. With respect to the flat plate, this uncertainty might be conservative due to the effects of changing the angle of attack. The angle of attack has no effect on the recovery factor in the continuum flow [84], while Oppenheim theory correctly predicts the influence of angle of attack on the recovery factor in the

free molecular regime [17, 85]. These two conclusions are important in predicting the effect of the angle of attack on the recovery factor in the slip and transition flow as can be seen in Eq. 76. Equation 77 was used to predict the recovery factor values in the slip and transition regimes. Examination of Eqs. 74 and 75 shows that the effect of the angle of attack is more severe at low speed than high speed (Fig. 22).

Figure 28 shows the variation of recovery factors at a fixed Mach number. The experiment [33] and theory confirm the fact that as Mach number becomes high, the recovery factor becomes lower for a cylinder. Figure 29 shows the trend that for decreasing Knudsen number, the recovery temperature ratio becomes smaller [33].
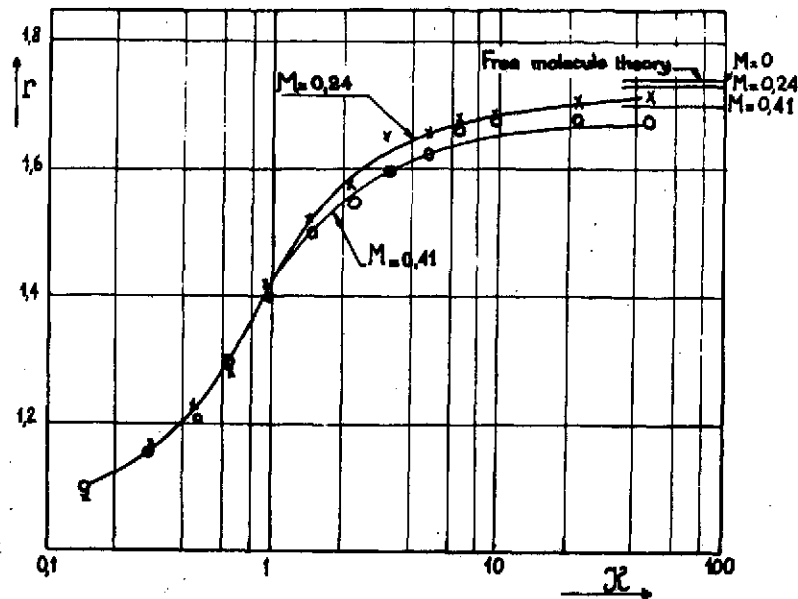
Fig. 28. Recovery factor versus Knudsen number at fixed Mach number. [21]
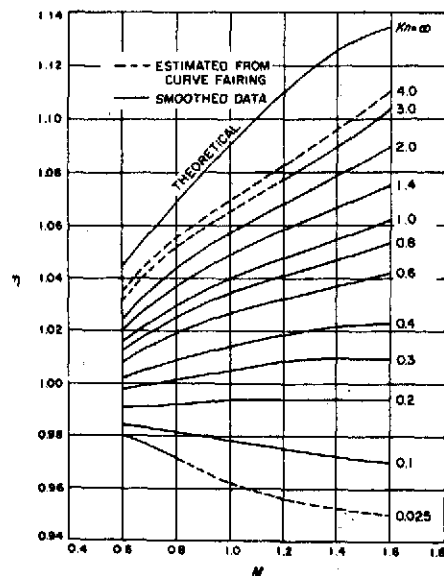
Fig. 29. Recovery temperature ratio versus Mach number at fixed Knudsen number. [33]

LIST OF REFERENCES

1. Schaff, S. A., and Chambre, P. L., *Flow of Rarefied Gases*, Princeton Aeronautical Paperbacks, Princeton University Press, 1961.

2. Hayes, W. D., and Probstein, R. F., *Hypersonic Flow Theory*, First Edition, Academic Press, New York, 1959.

3. Eckert, E. R. G., and Drake, D. M., Jr., *Heat and Mass Transfer*, McGraw-Hill Book Company, 1959.

4. Goldstein, S., *Modern Developments in Fluid Dynamics*, Vol. 2, Oxford University Press, New York, 1938.

5. Van Driest, E. R., "The Problem of Aerodynamics Heating," *Aeronautical Engineering Review*, October 1956.

6. Schlichting, H., *Boundary Layer Theory*, Sixth Edition, McGraw-Hill Book Company, 1968.

7. Eckert, E. R. G., *VDI-Forschungsheft*, 416, 1942.

8. Hilpert, R., "Wärmeahgabe Von Geheizten Drähten and Rohren in Luftstrom," Forsch, *Gebeite Ingenieurw*, Vol. 4, No. 215, 1933.

9. Grigull, U., and Gröber, H., *Grundgesetze der Wärmeübertragung*, Springer-Verlag, Berlin, 1955.

10. Kennard, E. H., *Kinetic Theory of Gases*, First Edition, McGraw-Hill Book Company, New York, 1938, pp. 291-335.

11. Sparrow, E. M., and Kinney, R. B., "Free Molecule Heat Transfer Between Parallel Plates," *The Physics of Fluids*, Vol. 7, No. 3, March 1964, pp. 473-475.

12. Wachman, H. Y., "The Thermal Accommodation Coefficient, A Critical Survey," *Journal of the American Rocket Society*, Vol. 32, No. 1, January 1962, pp. 2-12.

13. Springer, G. S., and Ratonyi, R., "Heat Conduction from Circular Cylinders in Rarefied Gases," *Journal of Heat Transfer*, Vol. 87, Series C, No. 4, November 1965, pp. 493-498.

14. Springer, G. S., and Wan, S. F., "Note on the Application of a Moment Method to Heat Conduction in Rarefied Gases Between Concentric Spheres," *AIAA Journal*, Vol. 4, No. 8, August 1966, pp. 1441-1443.

15. Su, C. L., and Willis, D. R., "Variational Principles for Heat Flux in a Rarefied Gas Between Concentric Cylinders," *The Physics of Fluids*, Vol. 11, No. 10, October 1968.

16. Oppenheim, A. K., "Generalized Theory of Convective Heat Transfer in a Free-Molecule Flow," *Journal of Aeronautical Sciences*, January 1953, pp. 49-58.

17. Stalder, J. R., Goodwin, G., and Creager, M. O., "Heat Transfer to Bodies in a High-Speed Rarefied-Gas Stream," NACA TN 2438, 1951.

18. Kovásznay, L. G., and Tormarek, E. I. A., *Heat Loss of Hot Wires in Supersonic Flow*, John Hopkins University Aeronautical Department, Bumblebee Report 127, April 1950.

19. Laufer, I., and McClellan, R., "Equilibrium Temperature and Heat Transfer Characteristics of Hot Wires in Supersonic Flow," GALCIT External Report 315, May 1956.

20. Shidlovskiy, V. P. E., *Introduction to Dynamics of Rarefied Gases*.

21. Atassi, H., and Brun, E. A., "Heat Transfer from Wires in a Rarefied Low Speed Flow," *Fifth International Symposium, Rarefied Gas Dynamics*, Vol. II, Academic Press, 1967, pp. 1221-1234.

22. Kogan, M. N., *Rarefied Gas Dynamics*, Academy of Science of the USSR, Moscow, Plenum Press, New York, 1969.

23. Talbot, L., "Free Molecular Flows and Heat Transfer for an Infinite Circular Cylinder at Angle of Attack," *Journal of Aerospace Science*, Vol. 24, No. 6, June 1957, pp. 458-459.

24. Sauer, F. M., "Convective Heat Transfer from Spheres in a Free Molecule Flow," *Journal of the Aeronautical Sciences*, Vol. 18, No. 5, May 1951, pp. 353-354.

25. Springer, G. S., *Heat Transfer in Rarefied Gas; A Survey*, University of Michigan, May 1969.

26. Bell, S., and Schaaf, S. A., "Heat Transfer to a Cylinder for the Free Molecule Flow of a Nonuniform Gas," *Jet Propulsion*, Vol. 25, No. 4, April 1955, pp. 168-169.

27. Touryan, K., and Maise, G., "Heat Transfer to a Sphere for Free Molecule Flow of a Nonuniform Gas," *AIAA Journal*, Vol. 1, No. 11, Nov. 1963, pp. 2644-2646.

28. Stalder, Jr. R., and Jukoff, O., "Heat Transfer to Bodies Traveling at High Speeds in the Upper Atmosphere," *Journal of Aerospace Science*, Vol. 15, No. 7, July 1948.

29. Abarbanel, S., "Radiative Heat Transfer in Free Molecule Flow," *Journal of Aerospace Science*, Vol. 28, No. 4, April 1961.

30. Sparrow, E. M., Johnson, V. K., Lundgren, T. S., Chen, T. S., "Heat Transfer and Forces for Free Molecule Flow on a Concave Cylindrical Surface," *Journal of Heat Transfer*, Vol. 86, Series C, No. 1, February 1964, pp. 1-11.

31. Schamberg, R., "On Concave Bodies in Free Molecule Flow," Report
     P-3164, Rand Corporation, Santa Monica, California, May 1965.

32. Chanine, M. T., "Free Molecule Flow Over Nonconvex Surfaces,"
     Rarefied Gas Dynamics, (L. Talbot, Editor), Academic Press, New
     York, 1961.

33. Vrebalovich, T., "Heat Loss and Recovery Temperature of Fine Wires
     in Transonic Transition Flow," *Fifth International Symposium,
     Rarefied Gass Dynamics*, Vol. II, Academic Press, 1967, pp. 1205-1219.

34. Sherman, F. S., "A Survey of Experimental Results and Methods for
     the Transition Regime of the Rarefied Gas Dynamics," *Rarefied Gas
     Dynamics Third Symposium*, Academic Press, New York, 1963.

35. Jaffé, G., *Ann. Physik*, 6, 195, 1930.

36. Takao, K., "Heat Transfer from a Sphere in a Rarefied Gas,"
     Rarefied Gas Dynamics (Lauermann, J. A., Editor), Vol. II, Academic
     Press, New York, 1963, pp. 102-111.

37. Heineman, M., *Commun. on Pure and Applied Math.*, 1, 259, 1948.

38. Keller, J., *Commun. on Pure and Applied Math.*, 1, 275, 1948.

39. Wang-Chang, C. S., and Uhlenbeck, G. E., "The Heat Transport between
     Two Parallel Plates as Functions of the Knudsen Number," University
     of Michigan Engineering Research Institute Report M999, 1953.

40. Kryzwoblocki, M. Z., and Shinasaki, G., *Acta Phys.*, Austriaca, 10,
     1956, pp 34-53.

41. Szymanski, Z., *Arch. Mech. Stosowanej*, 8, 1956.

42. Lunc, M., and Lubonski, J., *Arch. Mech. Stowanej*, 4, 1956, p. 597.

43. Kavanua, L. L., "Heat Transfer from Sphere to a Rarefied Gas in
     Subsonic Flow, *ASME Transaction*, Vol. 77, 1955.

44. Cybolski, R. J., and Baldwin, L. V., "Heat Transfer from Cylinders
     in Transition from Slip Flow to Free Molecular Flow," NASA Memo
     4-24-59E, May 1959.

45. Rott, N., and Lenard, M., "The Effect of Slip, Particularly for
     Highly Cooled Walls," *Journal of the Aerospace Science*, Vol. 29,
     No. 5, May 1962, pp. 591-595.

46. Kemp, N. H., "Vorticity Interaction at an Axisymmetric Stagnation
     Point in a Viscous Incompressible Fluid," *Journal of the Aerospace
     Science*, Vol. 26, No. 8, August 1959, pp. 543-544.

47. Herring, T. K., "The Boundary Layer Near the Stagnation Point in
     Hypersonic Flow Past a Sphere," *Journal of Fluid Mechanics*, Vol. 7,
     No. 2, February 1960, pp. 257-272.

48. Probstein, R. F., and Kemp, N. H., "Viscous Aerodynamics Characteristics in Hypersonic Rarefied Gas Flow," *Journal of Aerospace Science*, Vol. 27, No. 3, March 1960, pp. 174-192.

49. Ting, L., Ferri, A., and Zakkay, V., "Blunt Body Heat Transfer at Hypersonic Speed and Low Reynolds Numbers," *Journal of the Aerospace Science*, Vol. 28, No. 12, December 1961, pp. 962-971.

50. VanDyke, M., "A Review and Extension of Second Order Boundary Layer Theory," *Rarefied Gas Dynamics* (J. A. Lauermann, Editor), Vol. II, Academic Press, New York, 1963, pp. 212-227.

51. VanDyke, M., "Higher Approximations in Boundary Layer Theory, Part I, General Analysis," *Journal of Fluid Mechanics*, Vol. 14, October 1962.

52. VanDyke, M., "Higher Approximation in Boundary Layer Theory, Part II, Application to the Leading Edges," *Journal of Fluid Mechanics*, Vol. 14, December 1962.

53. Hickman, R. S., and Giedt, W. H., "Heat Transfer to the Hemisphere Cylinder at Low Reynolds Number, " *AIAA Journal*, Vol. 1, No. 3, March 1963, pp. 665-672.

54. Wilson, M. R., and Wittliff, C. E., "Low Density Stagnation Point Heat Transfer in Hypersonic Shock Tunnel," *Journal of American Rocket Society*, Vol. 22, No. 2, February 1962, pp. 275-276.

55. Potter, J. L., and Miller, J. T., "Total Heating Load on Blunt Axisymmetric Bodies in the Low Density Flow," *AIAA Journal*, Vol. 1, No. 2, February 1963, pp. 480-481.

56. Carden, W. H., "Heat Transfer in Nonequilibrium Dissociated Hypersonic Flow with Surface Catalysis and Second Order Effects," *AIAA Journal*, Vol. 4, No. 10, October 1966, pp. 1704-1711.

57. Oman, R. A., and Scheuing, R. A., "On Slip Flow Heat Transfer to a Flat Plate," *Journal of the Aerospace Science*, Vol. 26, No. 2, February 1959, pp. 126-127.

58. Burnett, D., *Proceedings of the London Math. Society*, 40, 382, 1935.

59. Grad, H., *Commun. on Pure and Applied Math.*, 2, 331, 1949.

60. Hirschfelder, J. O., Curtiss, C. F., and Bird, R. B., *Molecular Theory of Liquids*, John Wiley and Sons, 1954.

61. Patterson, G. N., *Molecular Flow of Gases*, John Wiley and Sons, 1956.

62. Enskog, D., *Arkiv Mat. Astron, Fysik*, Stockholm, 21, 1928.

63. Chapman, S., and Cowling, T. G., "The Mathematical Theory of Non-uniform Gases," Cambridge University Press, 1939.

64. Maxwell, J. C., *The Scientific Papers of James Clark Maxwell*, Vol. 2, Cambridge University Press, 1890.

65. Sparrow, E. M., and Lin, S. M., "Laminar Heat Transfer in Tubes Under Slip Flow Conditions," *Journal of Heat Transfer*, Vol. 84, Series C, No. 4, November 1962, pp. 363-369.

66. Inman, R. M., "Laminar Slip Flow Heat Transfer in a Parallel Plate Channel or a Round Tube with Uniform Wall Heating," NASA TN D-2393, August 1964.

67. Inman, R. M., "Heat Transfer for Laminar Slip Flow of a Rarefied Gas in a Parallel Plate Channel or a Circular Tube with Uniform Wall Temperature," NASA TN D-2313, November 1964.

68. Deissler, R. A., "An Analysis of Second Order Slip Flow and Temperature Jump Boundary Conditions for Rarefied Gases," IJHMT, Vol. 7, No. 7, June 1964, pp. 681-694.

69. Donaldson, C., "An Approximate Method for Estimating the Incompressible Laminar Layer Characteristics on a Flat Plate in Slipping Flow, NACA Research Memo L9C02, 1942.

70. Lin, T. C., and Schaff, S. A., "The Effect of Slip on Flow Near a Stagnation Point and in a Boundary Layer," NACA TN 2568, 1951.

71. Mirels, H., "Estimate of Slip Effect on Compressible Laminar Boundary Layer Skin Friction," NACA TN 2609, 1952.

72. Nonweiler, T., "The Laminar Boundary Layer in Slip Flow," College of Aeronautics, Cranfield, Dept. 62, November 1952.

73. Drake, R. M., and Kane, E. D., "A Summary of the Present Status of Heat Transfer in Rarefied Gases," Report No. HE-150-73, University of California, Berkeley, California, 1950.

74. Drake, R. M., Jr., and Backer, G. H., "Heat Transfer from Spheres to a Rarefied Gas in Supersonic Flow," *ASME Transaction*, Vol. 74, October 1952.

75. Sauer, F. M., and Drake, R. M., "Forced Convection Heat Transfer from Horizontal Cylinders in a Rarefied Gas," *Journal of the Aeronautical Sciences*, Vol. 20, No. 3, 1953, pp. 175-180.

76. Baldwin, L. V., "Slip-Flow Heat Transfer from Cylinders in Subsonic Air Streams," NACA TN 4369, April 1958.

77. *U. S. Standard Atmosphere*, 1966, Prepared by Environmental Science Service Administration, National Aeronautics and Space Administration, United States Air Force.

78. Christiansen, W. H., "Development and Calibration of Cold Wire Probe for Use in Shock Tube," GALCIT Memorandum, No. 62, 1961.

79. Eckert, E., and Drewitz, O., *Forsch. Gebeite Ingenieurw*, Vol. 11, No. 116, 1940.

80. Evvard, J. C., Burges, W. C., and Tucker, H., Institute of Aeronautical Science, Preprint 438, 1954.

81. Thomson, Donald C., "The Accuracy of Miniature Bead Thermistors in the Measurement of Upper Air Temperature," AFCRL-66-773, 1966.

82. Hottel, H. C., and Kalitinsky, A., "Temperature Measurements in High-Velocity Air Stream," *ASME Transaction*, Vol. 67, A-25, 1965.

83. Moffat, R. J., "Gas Temperature Measurement" from *Temperature, Its Measurement and Control in Science and Industry*, Vol. 3, Reinhold Publishing Corporation, 1962, pp. 553-571.

84. Schubuer, G. B., and Tchen, C. M., "Turbulent Flow, Section B," from *Turbulent Flows and Heat Transfer*, Princeton University Press, 1959.

85. Hartree, D. R., *Mem. and Proceedings, Manchester Lit. and Phil. Society*, 80, 85, 1935.

86. Haworth, D. R., "Heat Transfer Coefficients," Publication No. 136, Oklahoma State University, 1963.

87. Beckwith, I. E., and Gallagher, J. J., "Heat Transfer and Recovery Temperature on a Sphere with Laminar, Transitional and Turbulent Boundary Layers at Mach Numbers of 2.00 and 4.15," NACA TN 4125, December 1957.

88. Sparrow, E. M., and Kinney, R. B., "Free Molecule Heat Transfer Between Parallel Plates," *The Physics of Fluids*, Vol. 7, No. 3, March 1964, pp. 473-475.

89. Kovasznay, L. S. G., "Physical Measurements in Gas Dynamics and Combustion," Vol. IV, Princeton University Press, Princeton, New Jersey, 1954.

90. Mack, S. F., and Schaff, S. A., "Viscous Effects on Stagnation Point Temperatures," University of California Report HE-150-96, 1951.

91. Morrisey, J. E., private communications, Chief, Direct Sensing Techniques Branch, Aerospace Instrumentation Laboratory (OAR), L. G. Hanscom Field, Bedford, Massachusetts.

92. Koshmarov, Y. A., "Heat Transfer of a Sharp Cone in a Supersonic Rarefied Gas Flow," IJHMT, Vol. 9, Pergamon Press, 1966, pp. 951-957.

93. Kavanau, L. L., and Drake, R. M., Jr., Report No. HE-150-108, University of California, 1953.

94. Johnson, H. A., and Rubesin, M. W., *ASME Transaction,* 71, 1946, pp. 447-456.

95. Laurmann, J. A., "Experimental Investigation of the Flow About the Leading Edge of a Flat Plate," Report No. HE-150-126, University of California, Berkeley, California, 1954.

96. Schaaf, S. A., "Rarefied Gas Dynamics," *Applied Mechanics Surveys,* Spartan Book, 1966.

97. Rogers, E. W. E., and Berry, C. J., "Research at NPL on the Influence at Supersonic Speeds and Low Reynolds Numbers of Thick Laminar Boundary Layers," *Rarefied Gas Dynamics,* Vol. 1, J. H. de Leeuw, Academic Press, 1965.

98. Falkner, V. M., and Skan, S. W., "Some Approximate Solutions of the Boundary Layer Equations," British Aeronautical Research Council Reports, and Mem. 1314, April 1930.

99. Vidal, R. J., and Bartz, J. A., "Experimental Studies of Low-Density Effects in Hypersonic Wedge Flows," *Rarefied Gas Dynamics,* Vol. 1, J. H. de Leeuw, Editor, Academic Press, 1965.

100. Wallace, J. E., and Burke, A. F., "An Experimental Study of Surface and Flow Field Effects in Hypersonic Low Density Flow over a Flat Plate," *Rarefied Gas Dynamics,* Vol. 1, J. H. de Leeuw, Editor, Academic Press, 1965.

101. Mirels, H., NACA TN 2609, 1952.

102. Sather, N. F., and Kaku, Y. J., "A Molecular Model for Slip Flow," *The Trend in Engineering at the University of Washington,* Seattle, Washington, 17, 4, October 1965.

103. Kays, M. W., *Convective Heat and Mass Transfer,* McGraw-Hill Book Company, 1966.

104. Probstein, R. F., "Heat Transfer in Rarefied Gas Flow," *Research in Heat Transfer,* J. A. Clark, Editor, Pergamon Press, New York, 1963, pp. 33-60.

SUBJECT INDEX

Absorptivity of surface, 26
Accommodation, complete, 13
      coefficients, (see Momentum and thermal accommodation coefficients)
Accuracy, transition and slip flow regime, for sphere, 43, 44
      for cylinder, 46
   of recovery factor in continuum regime, for cylindrical body, 61
      for spherical body, 63
      for cones, 65
      for free molecule flow, 69
      for transition and slip flow, 77
   (see also Uncertainty)
Actual error, 63
Adiabatic recovery temperature, 23, 26
Adiabatic surface, 55
Adiabatic wall temperature, 19
Ambient altitude conditions, 62
Angle of attack, 20, 68
      local, 26
      zero, 27
Analogy of $Nu = Nu(Re, M)$, 31
Apparent Mach number, elimination of, 41
Asymptotically in the continuum limit, 41
Axial flow, 17

Bessel function of first order, 40
      modified, 18
Boltzmann, equation, 11
      linearized, 36
      constant, 26
Boundary condition, 36, 55
      for flat plate in transition and slip flow, 34, 35
      for temperature jump, 35, 36
Boundary layer, 34, 54
      concept for flat plate in continuum flow, 4, 5
      for cylinder in the continuum flow, 6, 7
      development of, 4
      for flat plate in continuum flow, 5
      for high velocity, 57
      laminar, for flat plate in continuum flow, 4, 55
      for low velocity, 57
      turbulent, for flat plate in continuum flow, 5, 58
Bunett equations, the order of, 35

Characteristic, length, 2, 13, 32
      dimension, 11
      quantity, 53
Collision, 32
      between molecules, 2, 3, 12
      between molecules and body (wall), 2, 3
      the number of, 3

Free molecule flow regime (continued)
      nonuniform gas, 26
      Oppenheim theory (see Oppenheim theory)
      review of theory, 14
      stagnation temperature, 24
      various geometrical shapes, 15, 16
Free stream condition, 37
Friction, 34
      internal, 55
      skin, 32, 37
Function ratio, 51

Gases, rarefied, 1, 2
      rarefied stream, 14
Gas constant, molecule, 12
Gas dynamics, rarefied, 1, 3
General effect of slip flow and temperature jump, 34
General formulation, 32
Generalization, 31
General trend, of uncertainty in rarefied subsonic flow, 51
      of recovery factor, 64

Heat conduction term, 36
Heat transfer, 24,34, 36, 38
      convective, for large Mach number, 26
   in cylindrical body, 6
      from sphere, 74
      in a laminar flow, 54
   by interpolation rule, 52
      measurement, 55
      to a body, 13
Heat transfer coefficient, 2, 3, 4, 5
      average, 9
      average, for sphere, 40
      convective, for transverse cylinder, 28
      for separated part, 8
      for sphere in subsonic flow, 27
      for turbulent flow, 5
      in free molecule flow over flat plate, cylinder, sphere, 17, 18
      local, 7, 8
      over flat plate, 4, 5
Heat transfer mechanism, 3
Heat transfer rate, convective, 19, 23
Hypersonic, (see Free molecule regime)
      in flat plate, 27

Inaccuracy, 40
      of interpolation rule, 53
Incident angle, 16
Inertia terms, 36
Initial conditions, 12
Interaction effect, 34

Interpolation, 1
      formula, 43, 51
      rule, 1, 27, 42, 44, 49, 51, 53
Introduction, 1
      free molecule regime, 11, 67
      heat transfer coefficient, 2
      recovery factor, 2, 54, 55
      transition and slip flow regime, 32, 73
Inviscid layer, 34

Kinetic theory, 31
Kinetic gas, 11
Knudsen number, 1, 3, 13, 31, 34, 46, 78, 79
      definition, 2
      function of, 76, 77
Knudsen's formula, 12

Laminar boundary layers, 8, 10, 59, 60, 63
Laminar flow, 59, 64
      over flat plate, 4, 36
Laminar recovery factor, 64
Laminar slip flow, 38
Laplace transformation, 37
Leading edge, 62
Linearized Boltzmann equation (see Boltzmann)
Local angle of attack, (see Angle of attack)
Local heat transfer coefficient (see Heat transfer coefficient)
Local mean free path (see Mean free path)
Location of flow separation, 10
Log-log scale, 43
Loss due to convection heat transfer, 19
Loss of quantitative information, 31
Low density (see Density)

Mach number, 15, 23, 31, 33, 39, 45, 48, 63, 68
      as a parameter, 31
      independence principle, 24
      limit of, 33
      unity, 61
      variation, 61
      very large, 24, 38, 71
      zero, 33
Macroscopic, 31
Maxwell-Boltzmann equation, 32
Maxwell distribution, 26
      of velocity function, 21, 32, 64
Maximum error (see Error)
Maximum uncertainty (see Uncertainty)
Mean free path, 2, 12, 32
      local, 33
Mean overheat (see Overheat)
Modified recovery factor (see Recovery factor)
Modified Stanton number (see Stanton number)

Rarefied, 1, 2
      gas flow, 48
      subsonic flow, 39
Rarefied flow, high speed, 24
Rayleigh problem, 36
Recovery factor, 54, 57, 67, 68, 71
      flat plate, 74, 75, 76
      for sphere and cylinder, 68
      for the particular situation, 58
      for the (laminar) supersonic and subsonic, 63
      for various cones, 63, 65
      in free molecule flow, 66
      modified, 23, 24, 68
      for sphere, 70, 74
      thermal, 66, 67, 71
Recovery ratio, normalized, 72
Recovery temperature, 54, 57, 58, 74
      mean, 54
Recovery temperature ratio, in transonic flow for cylinder, 74
Reemission, diffuse, 14
      specular, 14
Reference temperature, 59
Reference velocity, 9
Reference length, 9
Reynolds number, 1, 31, 33, 38, 39, 40, 46, 49
      critical, 5, 6, 11
      local, 4, 5, 8, 10

Shock wave, 33, 39
Skin friction, (see Friction)
Slip flow, 1, 3
Slip (flow) regime, 31, 32, 34, 51, 52
      boundary condition in, 35
      diatomic in, 34
      flat plate in, 35
      free stream condition for flat plate in, 36
      heat transfer rate of, 35
      Maxwell molecules in, 35
      monoatomic in, 35
      Stanton number in, 37
      supersonic, 40
Speed ratio, 23
Sphere, 10, 30, 39, 40 (see also Subsonic, heat transfer coefficient)
      average heat transfer coefficient of, 10
      average Nusselt number of, 38, 39
      modified recovery factor of, 11, 25
Stagnation condition, 54
Stagnation point, 5
Stanton number, 15, 20, 21, 33, 37
      experimental result of, 30
      limit of, 33
      modified, 19, 24, 25